



UNIVERSITÀ DI PARMA

ARCHIVIO DELLA RICERCA

University of Parma Research Repository

Hyaluronic acid - PVA films for the simultaneous delivery of dexamethasone and levofloxacin to ocular tissues

This is the peer reviewed version of the following article:

Original

Hyaluronic acid - PVA films for the simultaneous delivery of dexamethasone and levofloxacin to ocular tissues / Ghezzi, Martina; Ferraboschi, Ilaria; Fantini, Adriana; Pescina, Silvia; Padula, Cristina; Santi, Patrizia; Sissa, Cristina; Nicoli, Sara. - In: INTERNATIONAL JOURNAL OF PHARMACEUTICS. - ISSN 0378-5173. - 638:(2023), p. 122911. [10.1016/j.ijpharm.2023.122911]

Availability:

This version is available at: 11381/2945412 since: 2023-05-17T07:53:12Z

Publisher:

Elsevier

Published

DOI:10.1016/j.ijpharm.2023.122911

Terms of use:

Anyone can freely access the full text of works made available as "Open Access". Works made available

Publisher copyright

note finali coverpage

(Article begins on next page)

1 **Hyaluronic acid - PVA films for the simultaneous delivery of dexamethasone and levofloxacin to** 2 **ocular tissues**

3 Martina Ghezzi, Ilaria Ferraboschi, Adriana Fantini, Silvia Pescina, Cristina Padula, Patrizia Santi, Cristina
4 Sissa, Sara Nicoli
5

6 **Highlights**

- 7 • Polymeric films for simultaneous ocular delivery of lipophilic and hydrophilic drugs.
- 8 • Modified release platform for the reduction of administration frequency.
- 9 • Film swelling behavior modulation by varying polyvinyl alcohol degree of hydrolysis.
- 10 • Possible use of the film for both corneal application and transscleral delivery.

11 **Abstract**

12 Ocular drug delivery is challenging due to the poor drug penetration across ocular barriers and short
13 retention time of the formulation at the application site. Films, applied as inserts or implants, can be used to
14 increase residence time while controlling drug release. In this work, hydrophilic films made of hyaluronic acid
15 and two kinds of PVA were loaded with dexamethasone (included as hydroxypropylcyclodextrin complex)
16 and levofloxacin. This association represents one of the main treatments for the post cataract surgery
17 management, and it is also promising for eye infections with pain and inflammation. Films were
18 characterized in terms of swelling and drug release and were then applied to porcine eye bulbs and isolated
19 ocular tissues. Film swelling leads to the formation of either a gel (3D swelling) or a larger film (2D swelling)
20 depending on the type of PVA used. Films, prepared in an easy and scalable method, demonstrated high
21 loading capacity, controlled drug release and the capability to deliver dexamethasone and levofloxacin to the
22 cornea and across the sclera, to potentially target also the posterior eye segment. Overall, this device can be
23 considered a multipurpose delivery platform intended for the concomitant release of lipophilic and
24 hydrophilic drugs.
25

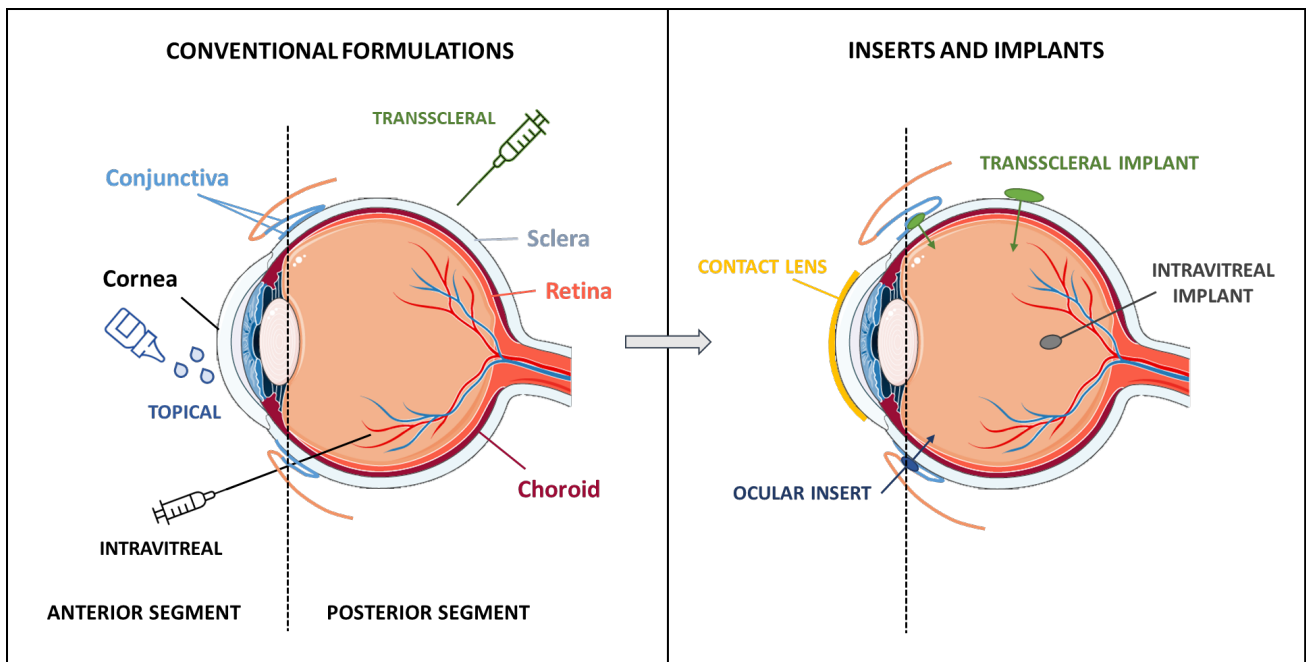
26 **Keywords**

27 Film; dexamethasone; levofloxacin; polyvinyl alcohol (PVA); hyaluronic acid, ocular delivery, insert
28

29 **1. Introduction**

30 Ocular drug delivery represents a real challenge due to the peculiar structure of the eye, characterized by
31 the presence of numerous static, dynamic and metabolic barriers. Ocular bioavailability is typically very low,
32 due to insufficient drug permeation across the ocular membranes and short retention time of the drug at the
33 application site (Lanier et al., 2021). For these reasons, this field is one of the most interesting for the research
34 in drug delivery, since the formulation can highly impact on the residence time at the application site and on
35 drug permeability across ocular tissues, dramatically changing the performance of a medication. Among the
36 numerous innovative vehicles, solid formulations, namely inserts and implants, answer predominantly to the
37 need of a reduction of the administration frequency, since they allow for increased residence time in the site
38 of application and a controlled release of the drug (Grassiri et al., 2021; Kompella et al., 2021). To highlight
39 the relevance of a reduced administration frequency, we can cite two emblematic examples: the need of
40 hourly drug application in the conjunctival sac in the treatment of some serious corneal infections (Lin et al.,
41 2019) and the need for lifetime intravitreal injection of corticosteroids and/or anti-VEGF compounds in the
42 treatment of some retinal diseases (Ghanchi et al., 2022). The reduction of the administration frequency is
43 of utmost importance: on one hand, it increases adherence to the treatment while, on the other hand, it

44 reduces fluctuations in drug tissues concentration and related side effects. Thus, both efficacy and patient's
45 compliance are increased. Despite the number of inserts and implants currently on the market is still not very
46 high, the research in this field is lively and concerns both the anterior and the posterior segment of the eye
47 (Alvarez-Lorenzo et al., 2019; Gaballa et al., 2021; Kim and Woo, 2021; Maulvi et al., 2021; Terreni et al.,
48 2020). As illustrated in Figure 1, controlled-release formulations can be inserted in the anterior segment of
49 the eye, namely in the conjunctival sac, in the lachrymal ducts or on the top of the cornea, as in case of
50 medicated contact lenses or implanted in the vitreous, in the subconjunctival/periocular space.
51



52
53 Figure 1. Main routes for drug delivery to the anterior and posterior eye segment and possible location of solid
54 controlled-release formulation. Figure modified with text, arrows and annotation after adaptation of “Eye” from Servier
55 Medical Art by Servier, licensed under a Creative Commons Attribution 3.0 Unported License
56 (<https://smart.servier.com>, accessed on 24 November 2022).
57

58 Dexamethasone (DEX) is one of the most potent corticosteroids used for the treatment of diseases affecting
59 both the anterior and the posterior eye segment (Gaballa et al., 2021). Its association with antibiotics is used
60 to treat eye infections which have pain and inflammation components, or, post-surgery, to prevent infections
61 and to treat the inflammation (Bandello et al., 2020; Rizzo et al., 2022). The most frequent use of this drug
62 combination is after cataract surgery, the most common surgical intervention worldwide. Corticosteroids
63 and antibiotics (sometimes also combined with NSADs) are generally applied 4 times a day, and a 5-minute
64 interval between the administration of different eye drops should be respected. This results in a complex
65 schedule and low adherence to the treatment (Matossian, 2020). To address, at least in part, this problem,
66 a new eye drop formulation containing 1 mg/mL DEX and 5 mg/mL levofloxacin (LVX), a broad-spectrum
67 fluoroquinolone antibiotic (Keating, 2009), was recently authorized in several European countries (EMA,
68 2022; Rizzo et al., 2022). This combination could simplify the therapy also reducing the danger for antibiotic
69 resistance. However, administration frequency is high (1 drop every 6 h) (Rizzo et al., 2022) and appropriate
70 eye-drop instillation remains a challenge (Matossian, 2020). Recent data suggest that a drop-free approach
71 could improve outcomes and the patient experience (Assil et al., 2021).

72 The aim of this work was the development, characterization and ex-vivo evaluation of an ocular film for the
73 controlled release of DEX and LVX. This combination could be useful for post-cataract management, but also
74 for posterior segment diseases, in the treatment of inflammatory conditions which can involve bacterial

75 infections (Gaballa et al., 2021; Prieto et al., 2020; Wang et al., 2013). Excipients used for the preparation
76 were hyaluronic acid (HA) and polyvinyl alcohol (PVA). Polymeric films containing PVA or HA have been
77 previously investigated as ocular drug delivery systems: PVA is well known for its excellent film-forming
78 properties and has been used, for instance, in combination with PVP to prepare films for the ocular release
79 of progesterone (Alambiaga-Caravaca et al., 2021). A timolol-loaded film composed of hyaluronic acid and
80 hydroxypropyl methylcellulose demonstrated biocompatibility and an extended-release profile
81 (Tighsazzadeh et al., 2019); a novel hyaluronic acid membrane showed its usefulness for the treatment of
82 ocular surface diseases by promoting corneal epithelium healing (Kim et al., 2021), whereas a
83 dexamethasone-loaded film made of hyaluronic acid and itraconic acid demonstrated to reduce IL-6
84 production by TNF- α inflamed corneal epithelial cells (Calles et al., 2016). Recently, Bao et al prepared
85 hydrogel films for the combined delivery of dexamethasone and levofloxacin; the system, made of oxidized
86 hyaluronic acid and dexamethasone covalently conjugated with glycol chitosan, showed to be promising for
87 the treatment of postoperative endophthalmitis [50]. In this work, HA and PVA were combined and PVA
88 hydrolysis degree was exploited to modulate swelling properties (2D or 3D) of the film and tailor its
89 characteristics to the application in different eye compartments. Additionally, with respect to previous
90 works, a delivery platform for the simultaneous delivery of an hydrophilic and a lipophilic drug was
91 developed, using an easy and potentially scalable method, and excipients approved for ocular administration.
92 After an initial screening phase, two polymeric compositions were selected: both contained HA and differed
93 for the presence of two kinds of PVA, characterized by similar molecular weight (MW), but different
94 hydrolysis grade. As DEX is a poorly water-soluble drug, its loading in the hydrophilic films was possible thanks
95 to the inclusion in cyclodextrins. Films were characterized in terms of swelling and drug release. They were
96 then applied to the porcine ocular tissues (namely cornea, sclera and the trilayer sclera-choiroid Bruch's
97 membrane) using validated ex-vivo models, to evaluate their capability to deliver the two drugs to the ocular
98 structures. Moreover, in order to figure-out if dexamethasone penetrates the tissue alone or included in
99 cyclodextrins, some films loaded with Nile-red-cyclodextrin complex were prepared and applied to ocular
100 tissues, which were then analysed by two-photon microscopy (Helmchen and Denk, 2005).

101 **2. Material and Methods**

102 **2.1. Materials**

103 Dexamethasone (DEX; IUPAC name: (8S,9R,10S,11S,13S,14S,16R,17R)-9-fluoro-11,17-dihydroxy-17-(2-
104 hydroxyacetyl)-10,13,16-trimethyl-6,7,8,11,12,14,15,16-octahydrocyclopenta[a]phenanthrene-3-one; MW:
105 392.5 g/mol; logP 1.83) was purchased from AlfaAesar (Karlsruhe, Germany) while levofloxacin (LVX; IUPAC
106 name: (2S)-7-fluoro-2-methyl-6-(4-methylpiperazin-1-yl)-10-oxo-4-oxa-1-azatricyclo[7.3.1.0^{5,13}]trideca-
107 5(13),6,8,11-tetraene-11-carboxylic acid; MW: 361.4 Da; pKa 5.2, 6.2, 8.2) was bought from Sigma-Aldrich
108 (St. Louis, MO, USA). Polyvinyl alcohol (PVA87; EG-25, MW: 83.4 kDa, hydrolysis degree: 86.5–89.0 mol%)
109 was purchased from Gohsei (Japan); polyvinyl alcohol (PVA98; MW: 72 kDa, hydrolysis degree: 97.5–
110 99.5 mol%) was from Fluka (Sigma-Aldrich, St. Louis, MO, USA). Sodium hyaluronate (HA; MW: 1000 kDa and
111 300 kDa) was from IBSA Farmaceutici S.p.A. (Lodi, Italy). Hydroxypropyl β -cyclodextrin (Kleptose[®]; HPCD;
112 MW: 1391 g/mol) was kindly provided by Roquette (Lestrem, France). Figure 2 illustrates the structure of HA,
113 PVA and HPCD. PEG400 (poly(ethylene glycol); MW: 380-420 g/mol) was purchased from Eigenmann &
114 Veronelli S.p.A. (Milano, Italy), whereas glycerin was bought from Merck (Darmstadt, Germany). Nile red (NR;
115 9-(diethylamino)-5H-benzo[a]phenoxazin-5-one; MW 318.4 g/mol) was purchased from Sigma Aldrich (St.
116 Louis, MO, USA).
117 For analysis, HPLC-grade acetonitrile and high purity water (Arium[®] comfort, Sartorius, Goettingen,
118 Germany) were used. All other chemicals were of analytical grade.

154 2.4. Films preparation

155 2.4.1. Blank films

156 To obtain the polymeric films, 2.5% w/w HA (300 or 1000 kDa) solutions and 15% w/w PVA (with hydrolysis
157 grade of either 87% or 98%) solutions were prepared and mixed in different ratios (see composition details
158 in Table S1). The method was modified from the method previously described by Padula et al (Padula et al.,
159 2007). Briefly, polymeric solutions were prepared separately by adding the polymer to high purity water
160 under magnetic stirring (100 rpm) at room temperature. In the case of PVA98, the dispersion in water was
161 heated at 90°C to get an homogeneous solution; the amount of water lost during heating was restored. The
162 prepared polymer solutions were carefully mixed (100 rpm) and the plasticizer (either glycerin or PEG 400)
163 was added to the final mixture by gently stirring. The obtained mixtures were left to stand for 24 h, then they
164 were spread on a glass plate using a film casting knife (BYK Gardner, Silversprings, MD, USA) with a gap of 2
165 mm, and oven-dried at 70°C for 1 hour. The composition of the films prepared is illustrated in Table S1. The
166 optimized formulations (87 and 98 in Table 1) were further loaded with drugs.

168 2.4.2. Films loaded with dexamethasone and levofloxacin

169 Formulations 87 and 98 were loaded with drugs. To solubilize DEX in the hydrophilic mixture, hydroxypropyl-
170 β -cyclodextrin (HPCD) was used.

171 Eight mg of DEX were dissolved in 4 mL of water containing 123 mg of HPCD. LVX (40 mg) was subsequently
172 added. The obtained solution was used for HA hydration (final conc. 2.5% w/w). Finally, 1 g of 15% w/w PVA
173 solutions and 28 mg of glycerin were added under gentle stirring until a homogeneous mixture was obtained.
174 The system was left to stand for at least 24 h to eliminate air bubbles, then spread on a glass plate using a
175 film casting knife with adjustable gap (BYK Gardner, Silversprings, MD, USA) that was set at 2 mm, and oven-
176 dried at 70°C for 1 hour.

177 Films containing only DEX were also prepared and, to investigate the possible role of HPCD in drug transport
178 across the cornea, DEX films containing higher HPCD amount (namely 246 mg) were prepared as well. In this
179 case, the film resulted very stiff and a higher amount of glycerin (140 mg) was necessary. Table 1 reports the
180 composition of the different mixtures used for film preparation, together with the codes used to identify the
181 films.

182
183 Table 1. Codification of the films and composition of the mixtures used for their preparation (wet basis).

CODE	Amount (mg) of each component in the mixture						
	PVA	HA	Glycerin	Water	DEX	LEVO	HPCD
87	150 (PVA87)	105	28	4000	-	-	-
98	150 (PVA98)	105	28	4000	-	-	-
87_βDL	150 (PVA87)	105	28	4000	8	40	123
98_βDL	150 (PVA98)	105	28	4000	8	40	123
87_βD	150 (PVA87)	105	28	4000	8	-	123
98_βD	150 (PVA98)	105	28	4000	8	-	123
87_ββD	150 (PVA87)	105	140	4000	8	-	246

184

185

186 2.5. Films characterization

187 2.5.1. Film swelling behaviour

188 Circular samples (0.6 cm²) were cut from each film, placed on a glass support and wet with 250 μ l of STF
189 heated at 37 °C. Pictures were taken with a camera (Nokia Lumia 630) after 0, 5, 10, 15 and 20 minutes
190 together with a reference area (A_R), and analyzed using ImageJ software (ImageJ 1.52q, NIH, USA).

191

192 **2.5.2. Dexamethasone and levofloxacin content in the films**

193 Three circles (0.6 cm²) were cut from each loaded film. Each sample was measured for weight and thickness
194 (Absolute Digimatic 547-401, Mitutoyo, Milan, I, resolution 0.001 mm), immersed in 7 mL of high purity water
195 and stirred for 24 h at room temperature until complete dissolution. One mL of the solution was then
196 sampled, centrifuged for 10 minutes at 8000 rpm and analysed by HPLC in order to determine the amount of
197 DEX and LVX contained in the film. The results are expressed as % of drug (w/w) and as µg/cm².

198

199 **2.5.3. Dexamethasone and levofloxacin release from the films**

200 The experiment was performed at room temperature (19–22 °C). The set-up used, previously published
201 (Pescina et al., 2017), was a slight modification of the method described by Sandri et al (Sandri et al., 2010).
202 Film circles (0.6 cm²) were applied to a 9 cm diameter glass Petri dish inclined at 45°. Then, simulated tear
203 fluid was flushed onto the film using a syringe pump (Harvard Apparatus, Holliston, MA) set at 0.06 mL/min
204 flow-rate. The solution was collected at predetermined time points up to 4 h and analyzed by HPLC for the
205 determination of DEX and LVX released. Release studies were carried out for the films 87_βD, 87_βDL,
206 87_ββD, 98_βD and 98_βDL.

207

208 **2.6. Dexamethasone and levofloxacin permeation across ocular tissues**

209 **2.6.1. Tissue preparation**

210 Porcine eyes were obtained from a local slaughterhouse within 3 h from animal death (pig breed, Large White
211 and Landrace; weight, 145-190 kg; age, 10–11 months; sex, male and female). Eye bulbs were transported
212 to the lab in PBS buffer; the adherent muscle and the conjunctiva were removed. Porcine eyes were either
213 used intact, or dissected to isolate the sclera or the trilayer sclera-choroid-Bruch's membrane. For corneal
214 experiments only bulbs with macroscopically intact corneas were employed, whereas eyes showing opaque
215 corneas were discarded. During the dissection to isolate sclera or trilayer, the anterior segment of the eye
216 was circumferentially cut behind the limbus and discarded. The vitreous was removed, the eye cup was cut
217 into two halves and retina and Retinal Pigment Epithelium (RPE) were removed by using a cotton swab to
218 obtain the trilayer composed of sclera, choroid and Bruch's layer. When the isolated sclera was used, the
219 choroid was eliminated by careful removal with tweezers.

220

221 **2.6.2. Uptake into the cornea**

222 To evaluate DEX and LVX uptake into the cornea, films 87_βD, 87_βDL, 87_ββD, 98_βD and 98_βDL
223 (composition in Table 1) were applied to the corneal surface of intact eye bulbs. The set-up used permits to
224 thermostat the eye at 37°C. Details of the set-up used are shown in the supplementary material (Figure S2).
225 Each film (0.6 cm²) was applied on the cornea after wetting the surface with STF. 10 µL of STF were further
226 added on the top of the film every hour, to maintain surface hydration. After 4 h of contact, the swollen
227 film/gel was removed, the cornea was carefully washed with high purity water and filter paper, and
228 subsequently isolated and transferred in an Eppendorf tube. The tissue was then extracted by addition of 1
229 mL of CH₃CN:H₂O (35:65, v:v) for 1.5 h at room temperature. After centrifugation (12000 rpm for 12 min),
230 the supernatant was sampled for the HPLC analysis and the tissue was extracted a second time (1 mL of
231 CH₃CN:H₂O (35:65, v:v); overnight). To calculate the drug accumulated in the tissue, the amount from the
232 first and second extractions were summed. This procedure was validated for DEX recovery, and the extracted
233 % resulted 100 ± 2.1 (approximately 82% in the first extraction and 18% in the second). This procedure was
234 also challenged for levofloxacin extraction; the recovery % obtained was 98 ± 6%. Each condition was
235 replicated 3 to 4 times.

236

237 **2.6.3. Permeation across the sclera and the trilayer (sclera-choiroid-Bruch's membrane)**

238 Permeation experiments were performed using vertical diffusion cells with an area of 0.6 cm². The scleral
239 tissue or the trilayer was clamped between the donor and the receptor compartments with the conjunctival
240 side facing the donor. The receptor compartment contained 4 mL of pH 7.4 PBS kept at 37 °C, and
241 magnetically stirred. Before film application (area 0.6 cm²), the sclera was wetted with 24 µL of PBS to favour
242 film adhesion to the tissue. The receiving solution was sampled every hour up to 6 (5 h in the case of the
243 trilayer) for the quantification of DEX and LVX permeated. The solubility of DEX in the receptor buffer was
244 determined and resulted enough to guarantee sink conditions (solubility: 55.78 ± 1.36 µg/mL). The films
245 tested were 87_βDL and 98_βDL for trans-scleral transport, while only 87_βDL for trilayer permeation.
246 The amount of drug permeated, normalized for the permeation area, was plotted against time and the flux J
247 (µg/cm² h) was calculated as the slope of the regression line after the achievement of the steady state.
248 The lag time is represented by the intercept of the regression line on the time axis. The permeability
249 coefficient P (cm/s) was calculated as $P = J/C_d$, where C_d (µg/mL) is the concentration of DEX or LVX in the
250 film (Table 2).

251

252 **2.7. Two-photon microscopy and fluorescence spectroscopy**

253 Nile red-loaded films based on PVA87 were prepared for the two-photon imaging: 123 mg of HPCD were
254 solubilized in 4 mL of water and added to 2 µL of a 10 mg/mL Nile red solution in DMSO. The obtained vehicle
255 was used for HA hydration, then the method was the same as in par 2.4.2., except for the absence of the two
256 drugs. The films were evaluated on corneal and scleral tissues, with the method previously described (par
257 2.6.2). Corneal and scleral tissues were mounted on Franz-type vertical diffusion cells (area 0.6 cm² for sclera
258 and 0.2 cm² for cornea). The experiment duration was 4 h. The samples were then frozen at -20°C until
259 microscopy analysis.

260 Corneal and scleral samples were analyzed with a Two-Photon Microscope Nikon A1R MP+ Upright coupled
261 with a femtosecond pulsed laser Coherent Chameleon Discovery (~ 100 fs pulse duration with 80 MHz
262 repetition rate, tunable wavelength output 660 - 1320 nm). A 25x water dipping objective with numerical
263 aperture 1.1 and 2.0 mm working distance was used to focus the excitation beam and to collect the two-
264 photon excited fluorescence (TPEF) and the second harmonic generation (SHG) signals. The outcoming signal
265 was directed by a dichroic mirror to two non-descanned detectors (high sensitivity GaAsP photomultiplier
266 tubes) allowing fast image acquisition. Optical filters preceded the detectors allowing the simultaneous
267 acquisition of two separated channels: green channel (506 - 593 nm) and red channel (604 - 679 nm). The
268 operation software of the microscope performed the overlay and the processing of the two channels images.
269 A third photomultiplier GaAsP detector, connected to the microscope through an optical fiber and preceded
270 by a dispersive element, was used to record emission spectra of the two-photon excited samples (wavelength
271 range 430-650 nm with a bandwidth of 10 nm).

272 Fluorescence measurements on liquid samples were performed with a FLS1000 Edinburgh Fluorometer.
273 Emission spectra were collected on diluted solutions, with absorbance lower than 0.1 to avoid inner filter
274 effects. All fluorescence spectra were duly corrected for the excitation intensity and the detector sensitivity.
275 For the preparation of NR solution in water, 20 µL of a 400 µM DMSO NR stock solution were added in 3 mL
276 of high purity water (final NR concentration 2.7 µM, total percentage of DMSO <1%) and then filtered
277 (hydrophilic PTFE, AISIMÔ 0.22 µm).

278

279 **2.8. Statistical analysis**

280 Results are expressed as the means of at least three experiments \pm standard deviation. Statistical analysis
281 was performed using Student's t test. The chosen level of significance was $p < 0.05$.

282

283

284 **3. Results and Discussion**

285 Several synthetic and natural polymers have been used for the preparation of inserts and implants and,
286 among them, hyaluronic acid (HA) and polyvinylalcohol (PVA) represent two examples of interest (Figure 2).
287 HA is a natural, biocompatible, biodegradable, hydrophilic and mucoadhesive polymer. It is widely used as
288 excipient, but it also shows lubricating and anti-dehydration properties, it showed to reduce the
289 inflammation caused by dryness and to stimulate the corneal re-epithelialization (Zhang et al., 2021). PVA is
290 a synthetic polymer with very good film-forming properties; it is produced from hydrolysis of polyvinyl
291 acetate and has been widely used in implantable and non-implantable devices demonstrating safety and
292 tolerability towards conjunctiva, cornea (Akbari et al., 2021; Li et al., 2015) and retina (Maruoka et al., 2006).
293 In this paper we combined the two polymers to prepare films for the ophthalmic delivery of two drugs,
294 namely DEX and LVX. Details regarding the screening phase carried out for optimizing the films are reported
295 in the Supplementary material section. At the end of the screening, two different films were selected (87 and
296 98 in Table 1); both contained a HA:PVA:glycerin ratio of 36:54:10 and differed for the hydrolysis grade of
297 the PVA used, that was either 87% (PVA87) or 98% (PVA98).

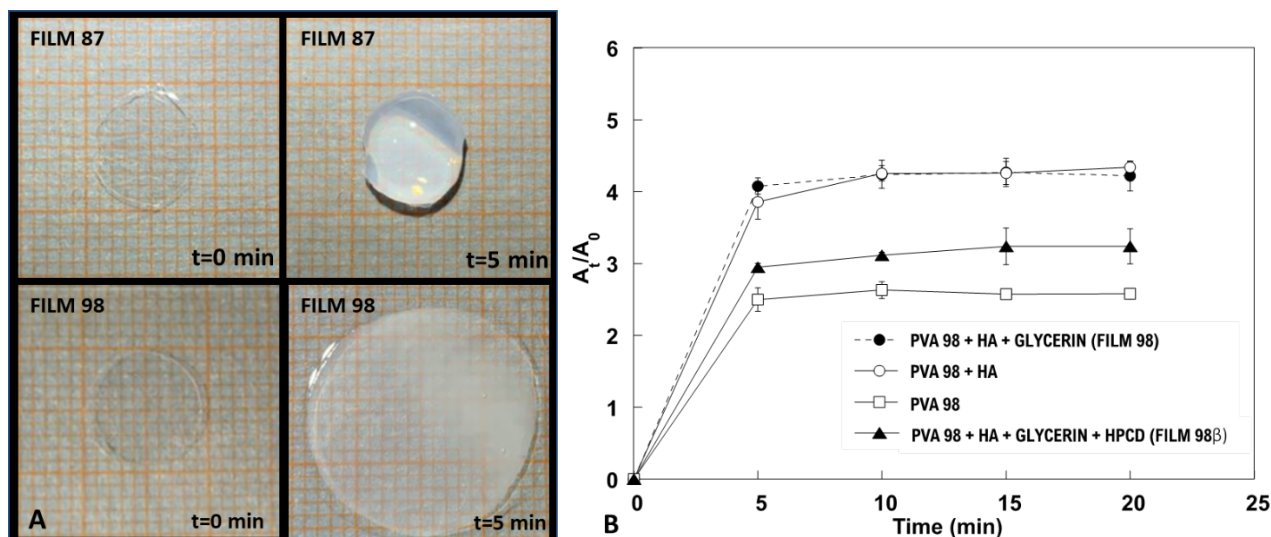
298

299 **3.1. Behavior of the films in contact with simulated tear fluid: swelling studies**

300 Upon ocular application, films will encounter tear fluid or interstitial fluids; thus, we evaluated the behavior
301 of the two selected films in contact with an aqueous buffer. As can be seen in Figure 3A, the film behaviour
302 highly depends upon the PVA used: films containing PVA87 swell three-dimensionally and then tend to
303 dissolve. The swelling behavior was not monitored since the gel is not enough compact to be sampled and
304 weighted. On the contrary, films containing PVA98 are characterized by a two-dimensional swelling (Figure
305 3A) which determines an increase in the surface of the film that can be monitored. PVA is produced from
306 hydrolysis of polyvinyl acetate and the hydrolysis grade refers to the % of acetate groups that has been
307 removed from the PVA chain (Figure 2); this parameter highly impacts on the physicochemical properties of
308 the polymer. For instance, a higher hydrolysis grade (PVA98) is associated to a higher possibility of inter- and
309 intra-chain H-bond formation, reflected in a lower water solubility (Morita et al., 2000). Analogously, the
310 different hydrolysis grade can also impact on PVA – HA interaction and on swelling behavior.

311 Figure 3B illustrates the area of the PVA98-based film, reported as A_t/A_0 ratio, as a function of time (A_0 =area
312 of the dry film; A_t =area of the film at time t after STF addition). To understand the contribution of all the
313 components, films made of PVA98 alone, PVA98 and HA (without glycerin), films of PVA98, HA and glycerin
314 and film also containing HPCD were evaluated.

315



316
 317 Figure 3. Panel A shows the appearance of the films based on PVA87 and PVA98 (HA:PVA:glycerin ratio of 36:54:10)
 318 after 5 minutes contact with simulated tear fluid. Panel B represents the 2D Swelling of PVA98-based films with various
 319 compositions.

320
 321 From Figure 3 it is evident that the swelling is very rapid as it occurs mainly in the first 5 minutes. From 10
 322 minutes onwards, there are no more substantial variations. The film containing only PVA (PVA 98) increases
 323 in area of about 2.5 times. By adding HA (PVA 98+HA), the swelling ratio increases to 4. Probably, the
 324 presence of HA reduces the PVA inter and intrachain interactions, favouring water uptake. The consequence
 325 is a higher relaxation of the PVA chains. Finally, the addition of glycerin (PVA 98+HA+GLYCERIN, FILM 98)
 326 does not substantially change the swelling behaviour. The swelling was evaluated also for films containing
 327 HPCD (PVA 98+HA+GLYCERIN+HPCD, FILM 98 β), since this compound has been used for DEX solubilization.
 328 The result highlights a reduction of the swelling extent, that could be ascribed to the formation of H-bonds
 329 between the external hydrophilic hydroxyl groups of CD and the two polymers, causing a reduction of
 330 polymer-water interaction and thus a reduction of the swelling.

331 In principle, the two-dimensional swelling could be useful in the case of corneal application, where the film
 332 could adhere to the tissue, protect a damaged epithelium and release the loaded drugs. This film is not
 333 supposed to behave as a contact lens but as a corneal bandage material.

334

335 3.2. Dexamethasone and levofloxacin-loaded polymeric films

336 Films 87 and 98 were then loaded with DEX and LVX. In order to load a lipophilic drug (DEX) into a hydrophilic
 337 film, a solubilizing strategy is needed. Among other, we decided to use cyclodextrins, cone-shaped
 338 oligosaccharides which are well known for their ability to solubilize hydrophobic compounds improving also
 339 their delivery to the tissues (Kristinsson et al., 1996; Shulman et al., 2015). Specifically, we used 3% w/w
 340 hydroxypropyl- β -cyclodextrin (HPCD) and found that DEX solubility increased 30 times, namely from $0.083 \pm$
 341 0.005 mg/mL to 2.52 ± 0.08 mg/mL, in agreement with literature data (Loftsson et al., 1994a). For the
 342 preparation of the final films, DEX was solubilized in 3% HPCD, the obtained solution was added to
 343 levofloxacin and then used to hydrate hyaluronic acid to prepare the final films (par 2.4.2). The exact
 344 composition of the mixtures prepared and laminated is reported in Table 1. The characteristics of the drug-
 345 loaded films in terms of weight, thickness and actual drug content are illustrated in Table 2.

346
 347 Table 2. Characteristics of the DEX and LVX-loaded dried films.

	Film properties	DEX content	LVX content
--	-----------------	-------------	-------------

	Weight (mg/cm ²)	Thickness (μm)	% w/w	μg/cm ²	% w/w	μg/cm ²
87_βDL	13.5 ± 0.49	100 ± 0.01	1.99 ± 0.08	262 ± 10	9.79 ± 0.51	1287 ± 66
98_βDL	12.78 ± 0.45	110 ± 0.02	2.01 ± 0.05	265 ± 6	8.90 ± 0.50	1170 ± 68

348

349 It is worth mentioning that the presence of cyclodextrin modified the characteristics of PVA98-based films,
350 reducing the 2D-swelling behavior (Figure 3B).

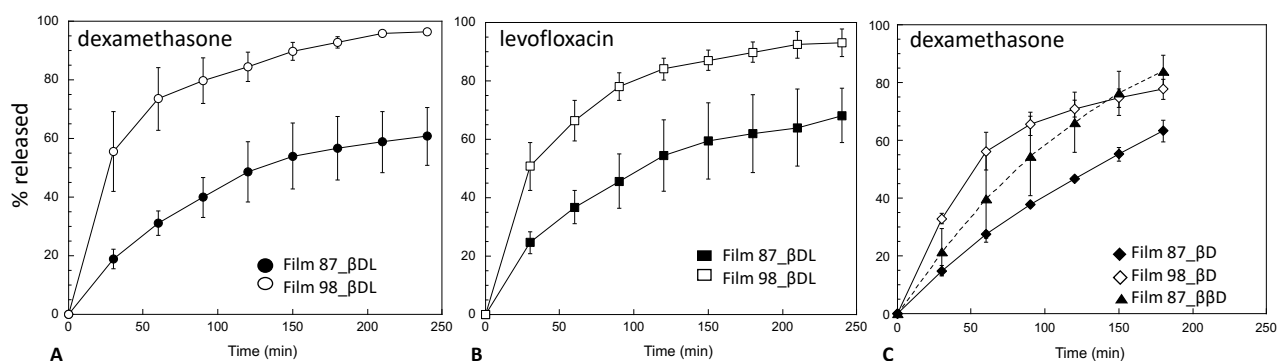
351

352 3.2.1. DEX and LVX release from the films

353 For the study of drug release from the films, a flow-through method where STF flows at 60 μl/min on the
354 formulation has been used. This method allows a slow contact of the formulation with water and, at the
355 same time, the mechanical action of fluid flow on the structure of the film, reproducing some of the
356 phenomena that take place after ocular application. Additionally, the plane is inclined at 45°, giving the
357 opportunity to evaluate the possible displacement of the film from the deposition site, thus inferring some
358 information on film adhesion properties. Indeed, none of the film have moved from the application position.

359 The results of DEX and LVX release from PVA87 and PVA98 based films are shown in Figure 4, panel A and B.

360



361

362 Figure 4. Release profiles obtained by using the inclined-plane set-up. Panel A and B report DEX and LVX release from
363 films 87_βDL and 98_βDL. Panel C shows the release from films containing only DEX (87_βD and 98_βD) also in the
364 presence of a doubled amount of HPCD (87_ββD).

365

366 The film containing PVA98 is characterized by a marked burst effect and a faster release than that containing
367 PVA87. For example, after 2 hours the film containing PVA87 released about 48% of DEX and 54% of LVX,
368 while the one containing PVA 98 released the 84% of both drugs. These differences are due to the different
369 degree of hydrolysis of the PVA which affects the structural characteristics of the film (Cascone et al., 2004;
370 Hdidar et al., 2017; Limpan et al., 2012). We can hypothesize that the presence of a higher proportion of
371 acetate groups in PVA87 limits the interactions with hyaluronic acid. Being scarcely involved in these bonds,
372 hyaluronic acid can better interact with water molecules, favoring a three-dimensional swelling of the film
373 and thus ensuring a slower and more controlled release of the active ingredients. On the other hand, in
374 PVA98 the higher degree of hydrolysis involves the presence of a greater number of free OH groups in the
375 polymer chains. This allows the polymer to interact more with hyaluronic acid which, being engaged in these
376 bonds, tends to have fewer interactions with water. This prevents the formation of the gel which is the
377 phenomenon that controls dexamethasone and levofloxacin release. An attempt to support this hypothesis
378 was done by quantifying hyaluronic acid released from the film; a published turbidimetric method (Oueslati
379 et al., 2014) was tried and validated in the presence of all other film components (Supplementary material,

380 Figure S1). Unfortunately, interactions between components taking place during film drying prevented an
381 accurate quantification of HA release, as detailed in the Supplementary material section.
382

383 In principle, these films could also be used for inflammatory diseases which do not need an antibiotic; for
384 this reason, the release of dexamethasone was studied also from films without levofloxacin. The result
385 obtained showed comparable profiles, even if film containing PVA98 showed lower variability and slightly
386 lower release (Figure 4, panel C). Finally, the impact of a higher cyclodextrin content was also evaluated
387 (Table 1) on PVA87 containing films, since cyclodextrin can have penetration enhancing properties and, for
388 this reason, this film was further evaluated on the cornea. In this case, the higher cyclodextrin content reflects
389 in a significantly faster drug release. We can hypothesize that in this film, that contains also a higher amount
390 of glycerin (see par 2.4.2), these two hydrophilic compounds interact with hydroxyl groups of HA, reducing
391 its interaction with water and thus the gel formation.

392 Overall, the release of the two drugs, obtained with the inclined plane set-up, is relatively fast. Nevertheless,
393 it should be highlighted that this method cannot closely reproduce the in vivo situation, characterized by the
394 presence of much lower fluid volumes. For instance, the volume contained in the conjunctival sac is about
395 7 μl and tears are produced with an average flow rate of 1–2 $\mu\text{l}/\text{mL}$ (Pepić et al., 2014; Van Haeringen, 1981);
396 even lower volumes and fluid movement are involved in case of subconjunctival space. The study of drug
397 release for ocular administration represents an important challenge and non-compendial apparatus and
398 conditions are often used (Adrianto et al., 2022; Pereira-da-Mota et al., 2022; Subrizi et al., 2019).
399

400 **3.3. Ocular applications of the prepared films**

401 Other authors previously demonstrated the interesting potential of solid platforms as films or contact lenses
402 for the delivery of dexamethasone (Balla et al., 2022; Bengani et al., 2020; Calles et al., 2016; Kim et al., 2010),
403 levofloxacin (Chang et al., 2022; Noori et al., 2021) or dexamethasone associated to one antibiotic (Baeyens
404 et al., 1998; Gade et al., 2020; Peng et al., 2010). Recently, Bao et al prepared hydrogel films for the combined
405 delivery of dexamethasone and levofloxacin; the system, made of oxidized hyaluronic acid and
406 dexamethasone covalently conjugated with glycol chitosan, showed to be promising for the treatment of
407 postoperative endophtalmitis (Bao et al., 2021).
408

409 **3.3.1. Targeting the anterior segment: drugs retention inside the cornea (intact eye-bulb model)**

410 To evaluate drug uptake into the cornea, the films were applied to the cornea surface of intact eye bulbs
411 (Figure S2). Given the mucoadhesive properties of the films, that can be attributed mainly to the presence of
412 hyaluronic acid, they adhered to the cornea throughout experiment duration, despite the regular addition
413 (every hour) of STF on their surface. The amount of drugs retained in the tissue is reported in Table 3 and
414 show no difference between the two films, that are able to accumulate approximately 10 μg of DEX and 90
415 μg of LVX per gram of cornea. This means that differences in the release kinetic do not reflect in a different
416 permeation probably because diffusion across corneal epithelium represents the limiting step to the
417 permeation. Despite this similarity, the behavior of the two films in contact with STF is very different (see
418 Figure 3A), and for this reason, the film containing PVA98 is more suitable for cornea application, while the
419 one with PVA87 could be better applied in the conjunctival sac. The accumulation of LVX (17-folds higher
420 with respect to DEX) cannot be simply explained by its higher concentration in the film. Probably, despite its
421 hydrophilicity the good penetration properties of LVX can be attributed to the presence of a carrier-mediated
422 transport in the epithelium (Kawazu et al., 1999).
423

424 Table 3. Amount of DEX and LVX accumulated in the cornea after 4 hours of application of the prepared film. The
 425 composition of the formulations is detailed in Table 1; the statistical analysis is summarized in Table S2.

Film	DEX		LVX	
	DEX ($\mu\text{g}/\text{cornea}$)	DEX ($\mu\text{g}/\text{g}$) ^a	LVX ($\mu\text{g}/\text{cornea}$)	LVX ($\mu\text{g}/\text{g}$) ^a
87_βDL	2.48 ± 1.55	10.77 ± 6.75	42.94 ± 2.48	186.80 ± 89.78
98_βDL	2.22 ± 0.79	9.65 ± 3.44	40.70 ± 2.22	176.97 ± 31.31
98_βD	3.18 ± 0.84	13.80 ± 3.64	-	-
87_βD	1.43 ± 0.23	6.23 ± 1.00	-	-
87_ββD	1.04 ± 0.35	4.52 ± 1.52	-	-

426 ^a Calculate by considering the average cornea weight : 230 ± 36 mg

427
 428 As far as we know there are not literature data on therapeutic concentration of DEX in the cornea for the
 429 treatment of inflammatory diseases. Even though, Djalilian et al. showed that cytokines production in human
 430 corneal epithelial cells and fibroblasts cell lines can be inhibited with a concentration of DEX 1 μM (0.392
 431 $\mu\text{g}/\text{mL}$) (Djalilian et al., 2006). As the amount of drug retained in the cornea from both films is at least 5-folds
 432 higher than the one required in vitro for cytokines inhibition, the formulations used could be considered
 433 promising. Also in case of levofloxacin, the cornea concentrations found largely exceed the MIC for *S. aureus*
 434 strains and for other frequent Gram-positive and Gram-negative eye pathogens (Dajcs Joseph et al., 2004;
 435 Figus et al., 2020; Yamaguchi et al., 2016). It is however worth mentioning that the experimental set-up used
 436 does not reproduce neither blinking nor the real rate of tear fluid production and drainage. These factors can
 437 be only studied in vivo, together with the evaluation of the actual mucoadhesive properties of the devices.
 438 Films containing DEX only were also evaluated. DEX-loaded films can be useful for the treatment of dry-eye
 439 disease (DED) since they could combine the anti-inflammatory action of DEX with HA, which in clinical studies
 440 showed to play a key role in reducing Dry Eye Disease (DED) symptoms (Yang et al., 2021). The amount of
 441 DEX accumulated resulted slightly higher (PVA98) or lower (PVA87) with respect to films containing also LVX,
 442 however, due to high data variability, differences are not statistically significant. Finally, since cyclodextrins
 443 are reported to promote drug transport across epithelia (Másson et al., 1999; Xu et al., 2021) and in particular
 444 across the cornea (Pescina et al., 2016), we prepared a film with a higher HPCD content (Table 1): DEX amount
 445 in the film was not increased in order to evaluate the ability of free HPCD (not involved in drug solubilisation)
 446 to interact with the corneal epithelium and increase its permeability. However, DEX accumulation did not
 447 improve (Table 3), resulting on the contrary in a small decrease, even if not statistically significant. The lack
 448 of enhancing activity of HPCD has been reported also by other authors (Babu et al., 2008; Loftsson et al.,
 449 1994b) and can be linked to the absence of free (i.e. not included in HPCD) drug in the film. Finally, it is worth
 450 highlighting that film 87_ββD is characterized by the lowest accumulation and the highest release rate (Figure
 451 4C), again indicating that the penetration into the tissue - and not the release from the film - accounts for
 452 the limiting step to the corneal accumulation.

453 Table S2 summarizes the result (p values) of the statistical analysis among the different conditions tested.

454
 455 **3.3.2. Targeting the posterior segment: permeation of dexamethasone and levofloxacin across the sclera**
 456 In principle, the prepared film could be applied below the conjunctiva (on the sclera surface) for the delivery
 457 of DEX to the posterior segment of the eye, for instance in the treatment of inflammatory conditions of the
 458 sclera, choroid, or retina (Beardsley et al., 2013; Gaballa et al., 2021; Nascimento et al., 2013; Prieto et al.,
 459 2020). The additional loading of LVX should be considered a plus in the management of some of these
 460 conditions, which can involve bacterial infections, usually resulting from antecedent traumas or surgical
 461 interventions (Beardsley et al., 2013; Tittler et al., 2012; Wang et al., 2013).

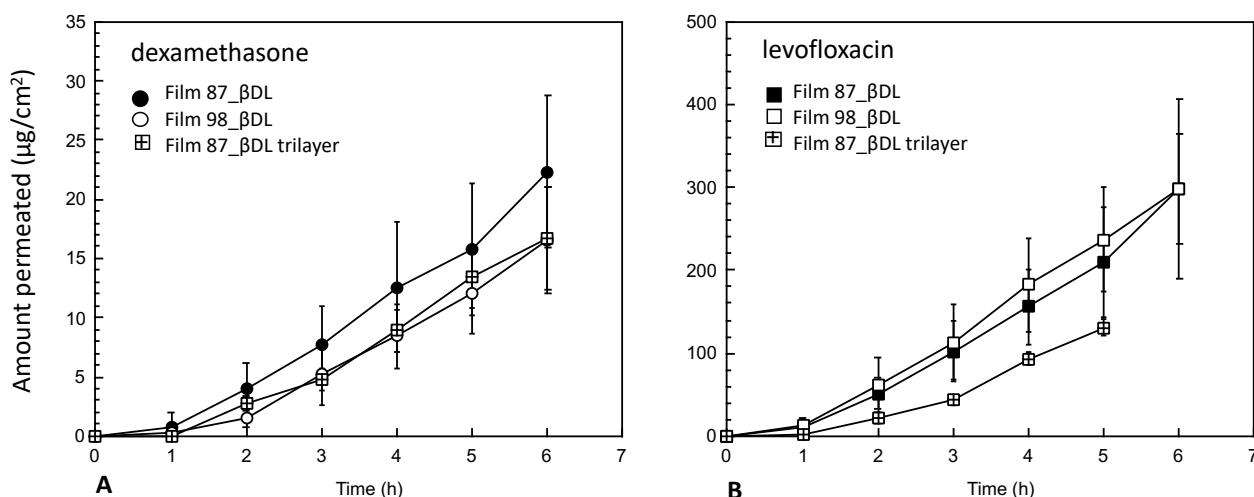


Figure 5. Permeation profiles of DEX (panel A) and LVX (panel B) from films of PVA87 and PVA98 across the sclera. The permeation across the trilayer sclera-choroid-Bruch's membrane from films of PVA87 is also shown.

The permeation profiles obtained for DEX and LVX from the two films are reported in Figure 5. In this case only combined films were evaluated, since the presence of LVX previously demonstrated a limited, if any, effect on DEX release and penetration. Permeation from both PVA87 and PVA98 based films have superimposable profiles for both drugs, although the release from the two films was considerably different. It is however important to underline that the set-up used in the two cases is different since the applied STF volume is different and thus drug release taking place in Franz cell can vary from the incline plane set-up.

Table 4 reports the permeation parameters obtained and highlights a 3-folds higher permeability coefficient of levofloxacin than dexamethasone. This is in agreement with the different nature of the two molecules: LVX is a hydrophilic amphoteric substance and diffusion across the hydrophilic interfibrillar matrix of the sclera is favoured, for comparison with DEX. Additionally, despite the similar MW, we cannot exclude that DEX is released from the film and penetrates inside the scleral pores as HPCD complex, i.e. the diffusion moiety will have a significantly higher MW. If compared with literature data, transscleral permeability coefficient of levofloxacin obtained in previous studies starting from a solution resulted 30-folds higher (approximately $5 \cdot 10^{-6}$ cm/s; (Pescina et al., 2012)) with respect to the permeation from the film, and the same can be said for dexamethasone: literature reports a permeability coefficient across porcine sclera of $11.1 \pm 2.1 \cdot 10^{-6}$ cm/s (Loch et al., 2012). This result supports a controlled release of the drugs from the formulations; indeed the % delivered through the sclera after 6 h was approx. 8% for DEX and 25% for LVX.

Table 4. Permeation parameters of DEX and LVX across sclera and trilayer.

Film	Tissue	Dexamethasone			Levofloxacin		
		J ($\mu\text{g}/\text{cm}^2\text{h}$)	$P \cdot 10^{-7}$ (cm/s)	Lag time (min)	J ($\mu\text{g}/\text{cm}^2\text{h}$)	$P \cdot 10^{-7}$ (cm/s)	Lag time (min)
87_βDL	Sclera	4.5 ± 1.1	0.63 ± 0.15^a	76 ± 20	55.1 ± 17.0	1.56 ± 0.48^a	68 ± 13
98_βDL	Sclera	4.0 ± 0.9	0.52 ± 0.13^a	117 ± 21	59.8 ± 9.0	1.86 ± 0.28^a	63 ± 27
87_βDL	Sclera-CHB	4.3 ± 0.9	0.61 ± 0.13^a	115 ± 5	36.7 ± 4.4	1.04 ± 0.12^a	87 ± 17

^a Calculated considering a drug concentration as in Table 2

489 Given the superimposable results obtained with the two different PVA across the sclera, only the film
490 composed of PVA87 (87_βDL), was evaluated across the trilayer (composed of sclera, choiroid and Bruch's
491 layer), in order to assess a possible contribution of melanin in the barrier properties of the tissue (Pescina et
492 al., 2012). However, as illustrated in Figure 5 no difference is present in comparison with permeation across
493 the sclera alone, suggesting that melanin does not represent a relevant barrier for DEX permeation. Indeed,
494 literature data suggest that DEX tendency to bind melanin is rather low (Rimpelä et al., 2020). On the
495 contrary, even if the differences are not statistically significant, a lower flux and longer lag time were seen in
496 case of levofloxacin, a compound characterized by a high affinity for melanin (Pescina et al., 2012). Overall,
497 the data collected support the use of this platform for the controlled delivery of DEX and LVX to the posterior
498 segment of the eye.

499

500 **3.4. Two-photon microscopy and fluorescence spectroscopy**

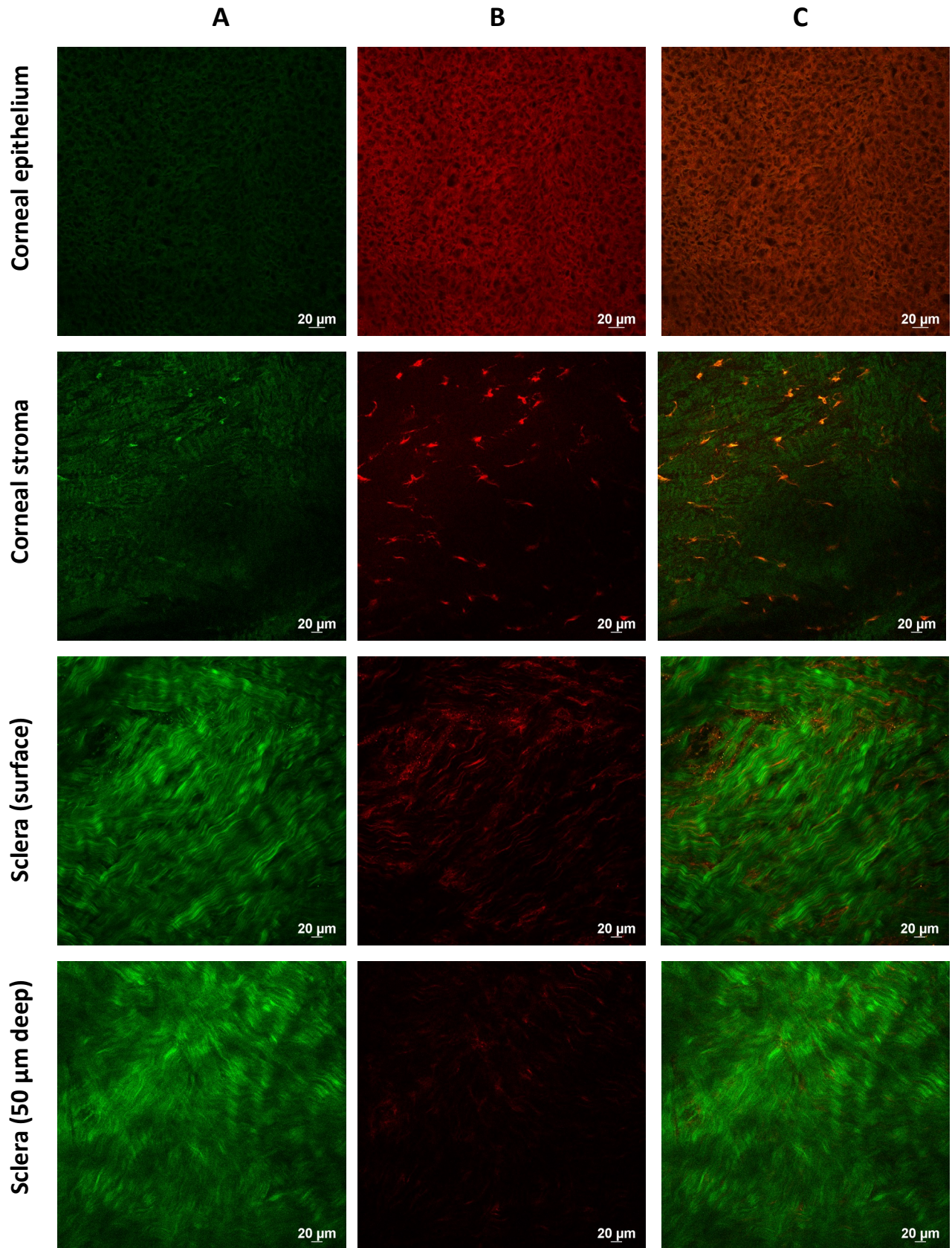
501 From the obtained data it is not possible to speculate if dexamethasone is released from the film as such or
502 included in the cyclodextrin and if the complex or dexamethasone alone penetrate into the tissues.

503 To figure out the possible penetration of the HPCD in the ocular tissues, Nile Red (NR) was solubilized in HPCD
504 and loaded in PVA87-based films. NR was selected since it is a fluorescent probe which shares with DEX a low
505 water solubility and a similar size (MW: 392.5 vs 318.4 Da). Additionally, the formation of an inclusion
506 complex between NR and HPCD has been reported in the literature (Hazra et al., 2004; Ray et al., 2019). NR-
507 loaded films were applied to cornea and sclera for 4 hours. Then, the tissues were imaged by two-photon
508 microscopy.

509

510 Figure 6 reports the images of the cornea (epithelium and stroma) and sclera upon excitation at 1100 nm.
511 The green signal presented in column A of Figure 6 can be mainly attributed to cell autofluorescence (Teng
512 et al., 2006) and Second Harmonic Generation (SHG) signal generated by collagen fibers (Teng et al., 2006;
513 Zyablitskaya et al., 2018), while the red signal (column B) corresponds to NR fluorescence; column C show
514 the image overlay. Overall, from Figure 6 we can assess that in the cornea, NR is clearly localized in cells, both
515 epithelial cells and fibroblasts of the stroma, while in the sclera, an inter-fiber localization can be envisaged.
516 It is not possible to extract quantitative information by comparing red intensity signal in the different tissues,
517 for two reasons: 1) the characteristics of the tissues are very different in terms of polarity, and NR emission
518 is affected by polarity of the environment (Kucherak et al., 2010); 2) the images were taken in slightly
519 different experimental conditions (see figure caption for details) to better visualize NR emission.

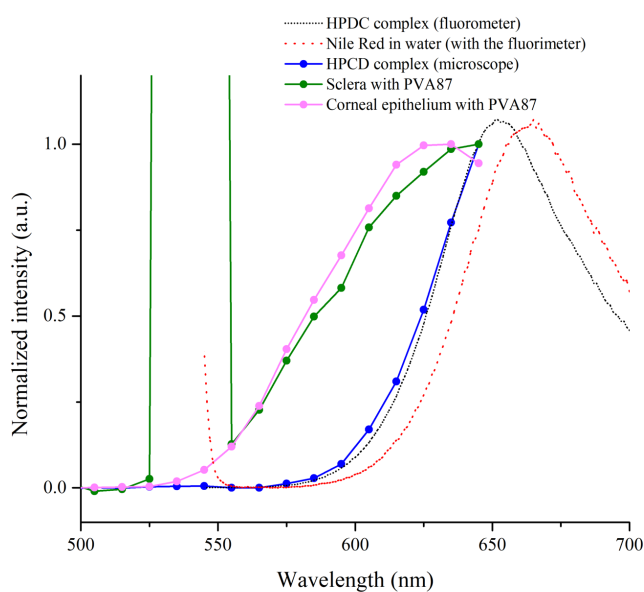
520



521
 522 Figure 6. Two-photon microscopy images obtained after tissue irradiation at 1100 nm. Tissues (cornea and sclera) were
 523 previously treated for 4 hours with a NR-loaded film (PVA87). Images show the corneal epithelium (Power laser: 1.5%.
 524 Green gain: 100. Red gain: 100), corneal stroma (150 μm depth from the endothelial surface; Power laser: 5%. Green
 525 gain: 150. Red gain: 150), sclera surface (Power laser: 1%. Green gain: 100. Red gain: 200) and sclera 50 μm deep from
 526 the episcleral surface (Power laser: 1%. Green gain: 100. Red gain: 200. Intensity of both channels increased with LUTs.).

527 Column A report the green signal, collected in the spectral region 506-593 nm. Green signal is due to cell
528 autofluorescence and SHG signal from collagen fibers. Column B report the red signal, collected in the spectral region
529 604 - 679 nm, which corresponds to NR fluorescence. Column C show overlay of images A and B. Holes visible in the
530 corneal epithelium are an artefact of the experimental procedure (i.e. tissue freezing after the permeation experiment).
531

532 Emission spectra were acquired to investigate the presence of HPCD complex in the tissue (Figure 7). In fact,
533 being NR a solvatochromic probe (Boldrini et al., 2002), the spectral position of its emission changes with the
534 polarity of the environment, allowing for the differentiation between NR included in the HPCD and NR
535 released from the HPCD. Figure 7 compares emission spectra of NR collected in different environment.
536 Emission of NR-HPCD complex in water (NR-HPDC, black dashed line in Figure 7) was collected with a
537 fluorometer (see section 2.7 for the instrument description), in order to detect the whole spectrum (the
538 spectral detector coupled with the microscope works in a limited spectral range from 400 nm to 650 nm):
539 the maximum of the emission band is detected at 650nm. The maximum of emission of NR in water is at 665
540 nm. The spectrum recorded from the corneal epithelium (Figure 7, pink line) is sizeably blue-shifted (25 nm)
541 compared to the spectrum of NR-HPDC complex, suggesting that NR has been released from HPCD and is
542 located in a less polar environment (Ghezzi et al., 2022). This is compatible with the probe localization inside
543 the lipophilic domains of the epithelial cells. A similar spectrum profile of NR is obtained also from the corneal
544 stroma (Supplementary Material, Figure S3), confirming that the NR-HPCD complex dissociates in contact
545 with the corneal surface or in the epithelial cells.



546 Figure 7. Emission spectra recorded in tissue samples and in solution. Spectra acquired with the fluorometer were
547 obtained exciting the sample at 540 nm, while spectra collected with the two-photon microscope were obtained exciting
548 the sample at 1080 nm, in order to minimize the tissue autofluorescence and maximize at the same time the NR signal.
549 Moreover, spectra collected with the two-photon microscope are collected up to 650 nm, since higher wavelengths fall
550 out of the detectable range of the instrument.
551

552
553 The spectral profile obtained from the sclera (50 μ m in depth from the surface) is slightly red-shifted
554 compared to corneal tissue and the maximum of its emission cannot be clearly detected (the same happens
555 for the NR-HPCD complex, when emission is detected with the spectral detector of the microscope, blue line
556 in Figure 7). Sclera is a strongly hydrophilic environment, and in case of release of NR from the HPDC, we
557 would expect an emission spectrum resembling emission in water (Ghezzi et al., 2022). Actually, emission of

558 NR appears to be blue-shifted with respect to NR emission in water: this result is in line with the hypothesis
559 that NR-HPCD complex diffuses (at least in part) intact in the interfibrillar matrix of the sclera. However, it is
560 difficult to give a definitive answer on the fate of the NR-HPDC complex within the scleral tissue, since the
561 spectral position and the shape of the emission band could to be influenced by the possible presence of the
562 other film components (HA, PVA and glycerin) that can likewise diffuse across the scleral pores affecting the
563 hydrophilicity of the environment in which NR is found.

564 **4. Conclusion**

565 In this work, a new delivery platform for the simultaneous delivery of hydrophilic and lipophilic drugs to eye
566 tissues was developed. The films, made of biocompatible polymers such as PVA and hyaluronic acid,
567 demonstrated high loading capacity with respect to both levofloxacin and dexamethasone. By changing the
568 hydrolysis grade of the PVA it was possible to modify the swelling behavior, thus adjusting the film
569 characteristics to the need of the specific application site in the eye: films made with PVA 98 and characterized
570 by a 2D swelling are more suitable for a corneal application, whereas in case of application in the conjunctival
571 sac or under the conjunctiva, film with a 3D swelling can be more easily used.

572 Films were prepared with an easy and potentially scalable method which did not involve the use of organic
573 solvents, furthermore all the excipients used are approved for ocular administration. Further investigations
574 are needed for a deeper comprehension of these systems concerning their behavior in an *in-vivo* condition
575 and to approach relevant issues such as mechanical properties, sterilization and stability. Preliminary data
576 indicate that both drugs are stable in the formulation for at least 6 months, but this aspect needs to be
577 investigated for longer time periods.

578 **5. Authors contributions**

579 All authors have read and agreed to the published version of the manuscript.

580 **6. Funding**

581 This work was supported by a Grant from the Italian Ministry for Education, University and Research (Grant
582 PRIN 2017 # 20173ZECCM Tackling biological barriers to antigen delivery by nanotechnological vaccines,
583 NanoTechVax). Iliaria Ferraboschi and Cristina Sissa benefited from the equipment and support of the COMP-
584 HUB Initiative, funded by the “Departments of Excellence” program of the Italian Ministry for Education,
585 University and Research (MIUR, 2018–2022). We acknowledge the financial support of the University of
586 Parma (Bando di accesso al Fondo Attrezzature Scientifiche 2018), for the purchase of the two-photon
587 microscopy facility. Iliaria Ferraboschi benefited of a PhD fellowship financed by PON R&I 2014–2020 (FSE
588 REACT-EU fundings). This work has received funding from the European Union's Horizon 2020 research and
589 innovation programme under the Marie Skłodowska-Curie grant agreement No 101007804 (Micro4Nano).

590 **7. CRediT authorship contribution statement**

591 **Martina Ghezzi:** Conceptualization, Methodology, Investigation, Writing – original draft, Writing – review &
592 editing. **Iliaria Ferraboschi:** Investigation, Writing – review & editing. **Adriana Fantini:** Methodology,
593 Investigation. **Silvia Pescina:** Methodology, Validation, Writing – review & editing. **Cristina**
594 **Padula:** Validation, Writing – review & editing. **Patrizia Santi:** Writing – review & editing, Funding
595 acquisition. **Cristina Sissa:** Validation, Writing – review & editing, Funding acquisition. **Sara**

596 **Nicoli:** Conceptualization, Methodology, Writing – original draft, Writing – review & editing, Funding
597 acquisition.

598 **8. Declaration of Competing Interests**

599 The authors declare that they have no known competing financial interests or personal relationships that
600 could have appeared to influence the work reported in this paper.

601
602 The paper has been partially presented at 4th European Conference on Pharmaceutics, 20 - 21 March 2023,
603 Marseille, France

604 **9. Acknowledgments**

605 Authors gratefully thank Pierugo Cavallini and Macello Annoni SpA for kindly providing porcine eye bulbs.
606 Former undergraduate students Cristiano Braga, Teresa Bagnaresi, Pamela Sofia and Vincenzo Minischetti
607 are gratefully acknowledged for their contribution in data collection.

608 **10. References**

- 609
610 Adrianto, M.F., Annuryanti, F., Wilson, C.G., Sheshala, R., Thakur, R.R.S., 2022. In vitro dissolution
611 testing models of ocular implants for posterior segment drug delivery. *Drug Delivery and*
612 *Translational Research* 12, 1355-1375. [10.1007/s13346-021-01043-z](https://doi.org/10.1007/s13346-021-01043-z)
- 613 Akbari, E., Imani, R., Shokrollahi, P., Heidari keshel, S., 2021. Preparation of Nanoparticle-Containing
614 Ring-Implanted Poly(Vinyl Alcohol) Contact Lens for Sustained Release of Hyaluronic Acid.
615 *Macromolecular Bioscience* 21, 2100043. <https://doi.org/10.1002/mabi.202100043>
- 616 Alambiaga-Caravaca, A.M., Domenech-Monsell, I.M., Sebastián-Morelló, M., Calatayud-Pascual,
617 M.A., Merino, V., Rodilla, V., López-Castellano, A., 2021. Development, characterization, and ex vivo
618 evaluation of an insert for the ocular administration of progesterone. *International Journal of*
619 *Pharmaceutics* 606, 120921. <https://doi.org/10.1016/j.ijpharm.2021.120921>
- 620 Alvarez-Lorenzo, C., Anguiano-Igea, S., Varela-García, A., Vivero-Lopez, M., Concheiro, A., 2019.
621 Bioinspired hydrogels for drug-eluting contact lenses. *Acta Biomaterialia* 84, 49-
622 62. <https://doi.org/10.1016/j.actbio.2018.11.020>
- 623 Assil, K.K., Greenwood, M.D., Gibson, A., Vantipalli, S., Metzinger, J.L., Goldstein, M.H., 2021.
624 Dropless cataract surgery: modernizing perioperative medical therapy to improve outcomes and
625 patient satisfaction. *Current Opinion in Ophthalmology* 32
- 626 Babu, R.J., Dayal, P., Singh, M., 2008. Effect of Cyclodextrins on the Complexation and Nasal
627 Permeation of Melatonin. *Drug Delivery* 15, 381-388. [10.1080/10717540802006922](https://doi.org/10.1080/10717540802006922)
- 628 Baeyens, V., Kaltsatos, V., Boisramé, B., Varesio, E., Veuthey, J.L., Fathi, M., Balant, L.P., Gex-Fabry,
629 M., Gurny, R., 1998. Optimized release of dexamethasone and gentamicin from a soluble ocular
630 insert for the treatment of external ophthalmic infections. *Journal of Controlled Release* 52, 215-
631 220. [https://doi.org/10.1016/S0168-3659\(97\)00212-5](https://doi.org/10.1016/S0168-3659(97)00212-5)
- 632 Balla, A., Ruponen, M., Valtari, A., Toropainen, E., Tuomainen, M., Alvarez-Lorenzo, C., del Amo,
633 E.M., Urtti, A., Vellonen, K.-S., 2022. Understanding dexamethasone kinetics in the rabbit tear fluid:
634 Drug release and clearance from solution, suspension and hydrogel formulations. *European Journal*
635 *of Pharmaceutics and Biopharmaceutics* 172, 53-60. <https://doi.org/10.1016/j.ejpb.2022.01.005>
- 636 Banello, F., Coassin, M., Di Zazzo, A., Rizzo, S., Biagini, I., Pozdeyeva, N., Sinitsyn, M., Verzin, A., De
637 Rosa, P., Calabrò, F., Avitabile, T., Bonfiglio, V., Fasce, F., Barraquer, R., Mateu, J.L., Kohnen, T.,
638 Carnovali, M., Malyugin, B., Aragona, P., Arvedi, P., Cagini, C., Caretti, L., Cavallini, G.M., Cillino, S.,

639 Figini, I., Franco, L.M., La Mantia, A., Laborante, A., Lanzetta, P., Marcigaglia, M., Mariotti, C.,
640 Martini, E., Mastropasqua, L., Morselli, S., Passani, F., Pece, A., Pertile, G., Pioppo, A., Pirondini, C.,
641 Pranterà, M., Rapisarda, A., Romano, M.R., Scarpa, G., Schiano-Lomoriello, D., Scordia, V., Scuderi,
642 G., Semeraro, F., Spedale, F., Staurengi, G., Tognetto, D., Tosi, M., Trabucchi, G., Trivella, F., Villani,
643 E., Vento, A., Vinciguerra, P., Alió, J.L., Alfonso Sanchez, J.F., Montiel, F.A., Lorenz, K., Panova, I.,
644 Eremina, A., Ciprandi, G., Group, L.-I., 2020. One week of levofloxacin plus dexamethasone eye
645 drops for cataract surgery: an innovative and rational therapeutic strategy. *Eye* 34, 2112-
646 2122. [10.1038/s41433-020-0869-1](https://doi.org/10.1038/s41433-020-0869-1)

647 Bao, Z., Yu, A., Shi, H., Hu, Y., Jin, B., Lin, D., Dai, M., Lei, L., Li, X., Wang, Y., 2021. Glycol
648 chitosan/oxidized hyaluronic acid hydrogel film for topical ocular delivery of dexamethasone and
649 levofloxacin. *International Journal of Biological Macromolecules* 167, 659-
650 666. <https://doi.org/10.1016/j.ijbiomac.2020.11.214>

651 Beardsley, R.M., Suhler, E.B., Rosenbaum, J.T., Lin, P., 2013. Pharmacotherapy of scleritis: current
652 paradigms and future directions. *Expert opinion on pharmacotherapy* 14, 411-
653 424. [10.1517/14656566.2013.772982](https://doi.org/10.1517/14656566.2013.772982)

654 Bengani, L.C., Kobashi, H., Ross, A.E., Zhai, H., Salvador-Culla, B., Tulsan, R., Kolovou, P.E., Mittal,
655 S.K., Chauhan, S.K., Kohane, D.S., Ciolino, J.B., 2020. Steroid-eluting contact lenses for corneal and
656 intraocular inflammation. *Acta Biomaterialia* 116, 149-
657 161. <https://doi.org/10.1016/j.actbio.2020.08.013>

658 Boldrini, B., Cavalli, E., Painelli, A., Terenziani, F., 2002. Polar Dyes in Solution: A Joint Experimental
659 and Theoretical Study of Absorption and Emission Band Shapes. *The Journal of Physical Chemistry*
660 *A* 106, 6286-6294. [10.1021/jp020031b](https://doi.org/10.1021/jp020031b)

661 Calles, J.A., López-García, A., Vallés, E.M., Palma, S.D., Diebold, Y., 2016. Preliminary characterization
662 of dexamethasone-loaded cross-linked hyaluronic acid films for topical ocular therapy. *International*
663 *Journal of Pharmaceutics* 509, 237-243. <https://doi.org/10.1016/j.ijpharm.2016.05.054>

664 Cascone, M.G., Lazzeri, L., Sparvoli, E., Scatena, M., Serino, L.P., Danti, S., 2004. Morphological
665 evaluation of bioartificial hydrogels as potential tissue engineering scaffolds. *Journal of Materials*
666 *Science: Materials in Medicine* 15, 1309-1313

667 Chang, Y.-F., Cheng, Y.-H., Ko, Y.-C., Chiou, S.-H., Jui-Ling Liu, C., 2022. Development of topical
668 chitosan/β-glycerophosphate-based hydrogel loaded with levofloxacin in the treatment of keratitis:
669 An ex-vivo study. *Heliyon* 8, e08697. <https://doi.org/10.1016/j.heliyon.2021.e08697>

670 Dajcs Joseph, J., Thibodeaux Brett, A., Marquart Mary, E., Girgis Dalia, O., Traidej, M., O'Callaghan
671 Richard, J., 2004. Effectiveness of Ciprofloxacin, Levofloxacin, or Moxifloxacin for Treatment of
672 Experimental *Staphylococcus aureus* Keratitis. *Antimicrobial Agents and Chemotherapy* 48, 1948-
673 1952. [10.1128/AAC.48.6.1948-1952.2004](https://doi.org/10.1128/AAC.48.6.1948-1952.2004)

674 Djalilian, A.R., Nagineni, C.N., Mahesh, S.P., Smith, J.A., Nussenblatt, R.B., Hooks, J.J., 2006.
675 Inhibition of Inflammatory Cytokine Production in Human Corneal Cells by Dexamethasone, but Not
676 Cyclosporin. *Cornea* 25

677 EMA, 2022. List of nationally authorized medicinal products. Duressa 1 mg/ml + 5 mg/ml, eye
678 drops, solution.

679 Figus, M., Posarelli, C., Romano, D., Nardi, M., Rossetti, L., 2020. Aqueous humour concentrations
680 after topical application of combined levofloxacin-dexamethasone eye drops and of its single
681 components: a randomized, assessor-blinded, parallel-group study in patients undergoing cataract
682 surgery: the iPERME study. *European Journal of Clinical Pharmacology* 76, 929-937. [10.1007/s00228-
683 020-02863-7](https://doi.org/10.1007/s00228-020-02863-7)

684 Gaballa, S.A., Kompella, U.B., Elgarhy, O., Alqahtani, A.M., Pierscionek, B., Alany, R.G., Abdelkader,
685 H., 2021. Corticosteroids in ophthalmology: drug delivery innovations, pharmacology, clinical

686 applications, and future perspectives. *Drug Delivery and Translational Research* 11, 866-
687 893.10.1007/s13346-020-00843-z

688 Gade, S.K., Nirmal, J., Garg, P., Venuganti, V.V.K., 2020. Corneal delivery of moxifloxacin and
689 dexamethasone combination using drug-eluting mucoadhesive contact lens to treat ocular
690 infections. *International Journal of Pharmaceutics* 591,
691 120023.<https://doi.org/10.1016/j.ijpharm.2020.120023>

692 Ghanchi, F., Bourne, R., Downes, S.M., Gale, R., Rennie, C., Tapply, I., Sivaprasad, S., 2022. An update
693 on long-acting therapies in chronic sight-threatening eye diseases of the posterior segment: AMD,
694 DMO, RVO, uveitis and glaucoma. *Eye (London, England)* 36, 1154-1167.10.1038/s41433-021-
695 01766-w

696 Ghezzi, M., Ferraboschi, I., Delledonne, A., Pescina, S., Padula, C., Santi, P., Sissa, C., Terenziani, F.,
697 Nicoli, S., 2022. Cyclosporine-loaded micelles for ocular delivery: Investigating the penetration
698 mechanisms. *Journal of Controlled Release* 349, 744-
699 755.<https://doi.org/10.1016/j.jconrel.2022.07.019>

700 Grassiri, B., Zambito, Y., Bernkop-Schnürch, A., 2021. Strategies to prolong the residence time of
701 drug delivery systems on ocular surface. *Advances in Colloid and Interface Science* 288,
702 102342.<https://doi.org/10.1016/j.cis.2020.102342>

703 Hazra, P., Chakrabarty, D., Chakraborty, A., Sarkar, N., 2004. Intramolecular charge transfer and
704 solvation dynamics of Nile Red in the nanocavity of cyclodextrins. *Chemical Physics Letters* 388, 150-
705 157.<https://doi.org/10.1016/j.cplett.2004.02.078>

706 Hdidar, M., Chouikhi, S., Fattoum, A., Arous, M., 2017. Effect of hydrolysis degree and mass
707 molecular weight on the structure and properties of PVA films. *Ionics* 23, 3125-
708 3135.10.1007/s11581-017-2103-0

709 Helmchen, F., Denk, W., 2005. Deep tissue two-photon microscopy. *Nature Methods* 2, 932-
710 940.10.1038/nmeth818

711 Kawazu, K., Midori, Y., Shiono, H., Ota, A., 1999. Characterization of the Carrier-mediated Transport
712 of Levofloxacin, a Fluoroquinolone Antimicrobial Agent, in Rabbit Cornea. *Journal of Pharmacy and*
713 *Pharmacology* 51, 797-801.10.1211/0022357991773168

714 Keating, G.M., 2009. Levofloxacin 0.5% Ophthalmic Solution. *Drugs* 69, 1267-
715 1286.10.2165/00003495-200969090-00009

716 Kim, D.J., Jung, M.-Y., Pak, H.-J., Park, J.-H., Kim, M., Chuck, R.S., Park, C.Y., 2021. Development of a
717 novel hyaluronic acid membrane for the treatment of ocular surface diseases. *Scientific Reports* 11,
718 2351.10.1038/s41598-021-81983-1

719 Kim, H.M., Woo, S.J., 2021. Ocular Drug Delivery to the Retina: Current Innovations and Future
720 Perspectives. *Pharmaceutics* 13, 108.10.3390/pharmaceutics13010108

721 Kim, J., Peng, C.-C., Chauhan, A., 2010. Extended release of dexamethasone from silicone-hydrogel
722 contact lenses containing vitamin E. *Journal of Controlled Release* 148, 110-
723 116.<https://doi.org/10.1016/j.jconrel.2010.07.119>

724 Kompella, U.B., Hartman, R.R., Patil, M.A., 2021. Extraocular, periorbital, and intraocular routes for
725 sustained drug delivery for glaucoma. *Prog. Retin. Eye Res.*
726 82.<https://doi.org/10.1016/j.preteyeres.2020.100901>

727 Kristinsson, J.K., Fridriksdóttir, H., Thórisdóttir, S., Sigurdardóttir, A.M., Stefánsson, E., Loftsson, T.,
728 1996. Dexamethasone-cyclodextrin-polymer co-complexes in aqueous eye drops. Aqueous humor
729 pharmacokinetics in humans. *Investigative Ophthalmology & Visual Science* 37, 1199-1203

730 Kucherak, O.A., Oncul, S., Darwich, Z., Yushchenko, D.A., Arntz, Y., Didier, P., Mély, Y., Klymchenko,
731 A.S., 2010. Switchable Nile Red-Based Probe for Cholesterol and Lipid Order at the Outer Leaflet of
732 Biomembranes. *Journal of the American Chemical Society* 132, 4907-4916.10.1021/ja100351w

733 Lanier, O.L., Manfre, M.G., Bailey, C., Liu, Z., Sparks, Z., Kulkarni, S., Chauhan, A., 2021. Review of
734 Approaches for Increasing Ophthalmic Bioavailability for Eye Drop Formulations. *AAPS*
735 *PharmSciTech* 22, 107.10.1208/s12249-021-01977-0

736 Li, G.-X., Gu, X., Song, H.-Y., Nan, K.-H., Chen, H., 2015. Biocompatibility and drug release behavior
737 of chitosan/poly (vinyl alcohol) corneal shield in vivo. *International journal of clinical and*
738 *experimental medicine* 8, 12949-12955

739 Limpan, N., Prodpran, T., Benjakul, S., Prasarpran, S., 2012. Influences of degree of hydrolysis and
740 molecular weight of poly(vinyl alcohol) (PVA) on properties of fish myofibrillar protein/PVA blend
741 films. *Food Hydrocolloids* 29, 226-233.<https://doi.org/10.1016/j.foodhyd.2012.03.007>

742 Lin, A., Rhee, M.K., Akpek, E.K., Amescua, G., Farid, M., Garcia-Ferrer, F.J., Varu, D.M., Musch, D.C.,
743 Dunn, S.P., Mah, F.S., 2019. Bacterial Keratitis Preferred Practice Pattern®. *Ophthalmology* 126, P1-
744 P55.<https://doi.org/10.1016/j.ophtha.2018.10.018>

745 Loch, C., Zakelj, S., Kristl, A., Nagel, S., Guthoff, R., Weitschies, W., Seidlitz, A., 2012. Determination
746 of permeability coefficients of ophthalmic drugs through different layers of porcine, rabbit and
747 bovine eyes. *European Journal of Pharmaceutical Sciences* 47, 131-
748 138.<https://doi.org/10.1016/j.ejps.2012.05.007>

749 Loftsson, T., Friðriksdóttir, H., Thórisdóttir, S., Stefánsson, E., 1994a. The effect of hydroxypropyl
750 methylcellulose on the release of dexamethasone from aqueous 2-hydroxypropyl- β -cyclodextrin
751 formulations. *International Journal of Pharmaceutics* 104, 181-184.[https://doi.org/10.1016/0378-5173\(94\)90194-5](https://doi.org/10.1016/0378-5173(94)90194-5)

752 Loftsson, T., Friðriksdóttir, H., Ingvarsdóttir, G., Jónsdóttir, B., Sigurðardóttir, A.M., 1994b. The
753 Influence of 2-Hydroxypropyl- β -Cyclodextrin on Diffusion Rates and Transdermal Delivery of
754 Hydrocortisone. *Drug Development and Industrial Pharmacy* 20, 1699-
755 1708.10.3109/03639049409050210

756 Maruoka, S., Matsuura, T., Kawasaki, K., Okamoto, M., Yoshiaki, H., Kodama, M., Sugiyama, M.,
757 Annaka, M., 2006. Biocompatibility of Polyvinylalcohol Gel as a Vitreous Substitute. *Current Eye*
758 *Research* 31, 599-606.10.1080/02713680600813854

759 Mátsson, M., Loftsson, T., Mátsson, G.s., Stefánsson, E., 1999. Cyclodextrins as permeation
760 enhancers: some theoretical evaluations and in vitro testing. *Journal of Controlled Release* 59, 107-
761 118.[https://doi.org/10.1016/S0168-3659\(98\)00182-5](https://doi.org/10.1016/S0168-3659(98)00182-5)

762 Matossian, C., 2020. Noncompliance with prescribed eyedrop regimens among patients undergoing
763 cataract surgery—prevalence, consequences, and solutions.

764 Maulvi, F.A., Desai, D.T., Shetty, K.H., Shah, D.O., Willcox, M.D.P., 2021. Advances and challenges in
765 the nanoparticles-laden contact lenses for ocular drug delivery. *International Journal of*
766 *Pharmaceutics* 608, 121090.<https://doi.org/10.1016/j.ijpharm.2021.121090>

767 Morita, R., Honda, R., Takahashi, Y., 2000. Development of oral controlled release preparations, a
768 PVA swelling controlled release system (SCRS): I. Design of SCRS and its release controlling factor.
769 *Journal of Controlled Release* 63, 297-304.[https://doi.org/10.1016/S0168-3659\(99\)00203-5](https://doi.org/10.1016/S0168-3659(99)00203-5)

770 Nascimento, H., França, M., García, L.G., Muccioli, C., Belfort, R., Jr., 2013. Subconjunctival
771 dexamethasone implant for non-necrotizing scleritis. *J Ophthalmic Inflamm Infect* 3, 7-
772 7.10.1186/1869-5760-3-7

773 Noori, M.M., Al-Shohani, A.D.H.H., Yousif, N.Z., 2021. Fabrication and characterization of new
774 combination ocular insert for the combined delivery of tinidazole and levofloxacin. *Materials Today:*
775 *Proceedings*.<https://doi.org/10.1016/j.matpr.2021.07.008>

776 Oueslati, N., Leblanc, P., Harscoat-Schiavo, C., Rondags, E., Meunier, S., Kapel, R., Marc, I., 2014.
777 CTAB turbidimetric method for assaying hyaluronic acid in complex environments and under cross-
778 linked form. *Carbohydrate Polymers* 112, 102-108.<https://doi.org/10.1016/j.carbpol.2014.05.039>

779

780 Padula, C., Nicoli S Fau - Aversa, V., Aversa V Fau - Colombo, P., Colombo P Fau - Falson, F., Falson F
781 Fau - Pirot, F., Pirot F Fau - Santi, P., Santi, P., 2007. Bioadhesive film for dermal and transdermal
782 drug delivery. *Eur. J. Dermatol.*, 4.10.1684/ejd.2007.0205
783 Peng, Y.-J., Kau, Y.-C., Wen, C.-W., Liu, K.-S., Liu, S.-J., 2010. Solvent-free biodegradable scleral plugs
784 providing sustained release of vancomycin, amikacin, and dexamethasone—An in vivo study.
785 *Journal of Biomedical Materials Research Part A* 94A, 426-432. <https://doi.org/10.1002/jbm.a.32697>
786 Pepić, I., Lovrić, J., Cetina-Čižmek, B., Reichl, S., Filipović-Grčić, J., 2014. Toward the practical
787 implementation of eye-related bioavailability prediction models. *Drug Discovery Today* 19, 31-
788 44. <https://doi.org/10.1016/j.drudis.2013.08.002>
789 Pereira-da-Mota, A.F., Phan, C.M., Concheiro, A., Jones, L., Alvarez-Lorenzo, C., 2022. Testing drug
790 release from medicated contact lenses: The missing link to predict in vivo performance. *Journal of*
791 *Controlled Release*. <https://doi.org/10.1016/j.jconrel.2022.02.014>
792 Pescina, S., Carra, F., Padula, C., Santi, P., Nicoli, S., 2016. Effect of pH and penetration enhancers
793 on cysteamine stability and trans-corneal transport. *European Journal of Pharmaceutics and*
794 *Biopharmaceutics* 107, 171-179. <https://doi.org/10.1016/j.ejpb.2016.07.009>
795 Pescina, S., Lucca, L.G., Govoni, P., Padula, C., Favero, E.D., Cantù, L., Santi, P., Nicoli, S., 2019. Ex
796 Vivo Conjunctival Retention and Transconjunctival Transport of Poorly Soluble Drugs Using
797 Polymeric Micelles. *Pharmaceutics* 11, 476.10.3390/pharmaceutics11090476
798 Pescina, S., Macaluso, C., Gioia, G.A., Padula, C., Santi, P., Nicoli, S., 2017. Mydriatics release from
799 solid and semi-solid ophthalmic formulations using different in vitro methods. *Drug Development*
800 *and Industrial Pharmacy* 43, 1472-1479.10.1080/03639045.2017.1318910
801 Pescina, S., Santi, P., Ferrari, G., Padula, C., Cavallini, P., Govoni, P., Nicoli, S., 2012. Ex vivo models
802 to evaluate the role of ocular melanin in trans-scleral drug delivery. *European Journal of*
803 *Pharmaceutical Sciences* 46, 475-483. <https://doi.org/10.1016/j.ejps.2012.03.013>
804 Prieto, E., Cardiel, M.J., Vispe, E.A.-O., Idoipe, M., Garcia-Martin, E., Fraile, J.M., Polo, V., Mayoral,
805 J.A., Pablo, L.E., Rodrigo, M.A.-O., 2020. Dexamethasone delivery to the ocular posterior segment
806 by sustained-release Laponite formulation. *Biomedical Materials* 15. 10.1088/1748-605X/aba445
807 Ray, A., Das, S., Chattopadhyay, N., 2019. Aggregation of Nile Red in Water: Prevention through
808 Encapsulation in β -Cyclodextrin. *ACS Omega* 4, 15-24.10.1021/acsomega.8b02503
809 Rimpelä, A.-K., Garneau, M., Baum-Kroker, K.S., Schönberger, T., Runge, F., Sauer, A., 2020.
810 Quantification of Drugs in Distinctly Separated Ocular Substructures of Albino and Pigmented Rats.
811 *Pharmaceutics* 12, 1174
812 Rizzo, S., Gambini, G., De Vico, U., Rizzo, C., Kilian, R., 2022. A One-Week Course of
813 Levofloxacin/Dexamethasone Eye Drops: A Review on a New Approach in Managing Patients After
814 Cataract Surgery. *Ophthalmol Ther* 11, 101-111.10.1007/s40123-021-00435-1
815 Sandri, G., Rossi, S., Ferrari, F., Bonferoni, M.C., Zerrouk, N., Caramella, C., 2010. Mucoadhesive and
816 penetration enhancement properties of three grades of hyaluronic acid using porcine buccal and
817 vaginal tissue, Caco-2 cell lines, and rat jejunum. *Journal of Pharmacy and Pharmacology* 56, 1083-
818 1090.10.1211/0022357044085
819 Shulman, S., Jóhannesson, G., Stefánsson, E., Loewenstein, A., Rosenblatt, A., Habet-Wilner, Z.,
820 2015. Topical dexamethasone-cyclodextrin nanoparticle eye drops for non-infectious Uveitic
821 macular oedema and vitritis – a pilot study. *Acta Ophthalmologica* 93, 411-
822 415. <https://doi.org/10.1111/aos.12744>
823 Subrizi, A., del Amo, E.M., Korzhikov-Vlakh, V., Tennikova, T., Ruponen, M., Urtti, A., 2019. Design
824 principles of ocular drug delivery systems: importance of drug payload, release rate, and material
825 properties. *Drug Discovery Today* 24, 1446-1457. <https://doi.org/10.1016/j.drudis.2019.02.001>
826 Teng, S.-W., Tan, H.-Y., Peng, J.-L., Lin, H.-H., Kim, K.H., Lo, W., Sun, Y., Lin, W.-C., Lin, S.-J., Jee, S.-
827 H., So, P.T.C., Dong, C.-Y., 2006. Multiphoton Autofluorescence and Second-Harmonic Generation

828 Imaging of the Ex Vivo Porcine Eye. *Investigative Ophthalmology & Visual Science* 47, 1216-
829 1224.10.1167/iovs.04-1520

830 Terreni, E., Burgalassi, S., Chetoni, P., Tampucci, S., Zucchetti, E., Fais, R., Ghelardi, E., Lupetti, A.,
831 Monti, D., 2020. Development and Characterization of a Novel Peptide-Loaded Antimicrobial Ocular
832 Insert. *Biomolecules* 10, 664.10.3390/biom10050664

833 Tighsazzadeh, M., Mitchell, J.C., Boateng, J.S., 2019. Development and evaluation of performance
834 characteristics of timolol-loaded composite ocular films as potential delivery platforms for
835 treatment of glaucoma. *International Journal of Pharmaceutics* 566, 111-
836 125.<https://doi.org/10.1016/j.ijpharm.2019.05.059>

837 Tittler, E.H., Nguyen, P., Rue, K.S., Vasconcelos-Santos, D.V., Song, J.C., Irvine, J.A., Smith, R.E., Rao,
838 N.A., Yiu, S.C., 2012. Early surgical debridement in the management of infectious scleritis after
839 pterygium excision. *J Ophthalmic Inflamm Infect* 2, 81-87.10.1007/s12348-012-0062-1

840 Van Haeringen, N.J., 1981. Clinical biochemistry of tears. *Survey of Ophthalmology* 26, 84-
841 96.[https://doi.org/10.1016/0039-6257\(81\)90145-4](https://doi.org/10.1016/0039-6257(81)90145-4)

842 Wang, T., Huang, X., Gao, Q., Feng, L., Xie, Z., Jiang, Z., Liu, Y., Li, Y., Lin, X., Lin, J., 2013. A Preliminary
843 Study to Treat Severe Endophthalmitis via a Foldable Capsular Vitreous Body with Sustained
844 Levofloxacin Release in Rabbits. *Investigative Ophthalmology & Visual Science* 54, 804-
845 812.10.1167/iovs.12-9695

846 Xu, C., Lu, J., Zhou, L., Liang, J., Fang, L., Cao, F., 2021. Multifunctional nanocomposite eye drops of
847 cyclodextrin complex@layered double hydroxides for relay drug delivery to the posterior segment
848 of the eye. *Carbohydrate Polymers* 260, 117800.<https://doi.org/10.1016/j.carbpol.2021.117800>

849 Yamaguchi, K., Tateda, K., Ohno, A., Ishii, Y., Murakami, H., 2016. [Surveillance of in vitro
850 susceptibilities to levofloxacin and various antibacterial agents for 11,762 clinical isolates obtained
851 from 69 centers in 2013]. *The Japanese Journal of Antibiotics*

852 Yang, Y.-J., Lee, W.-Y., Kim, Y.-J., Hong, Y.-P., 2021. A Meta-Analysis of the Efficacy of Hyaluronic Acid
853 Eye Drops for the Treatment of Dry Eye Syndrome. *International journal of environmental research
854 and public health* 18, 2383.10.3390/ijerph18052383

855 Zhang, X., Wei, D., Xu, Y., Zhu, Q., 2021. Hyaluronic acid in ocular drug delivery. *Carbohydrate
856 Polymers* 264, 118006.<https://doi.org/10.1016/j.carbpol.2021.118006>

857 Zyablitskaya, M., Munteanu, E.L., Nagasaki, T., Paik, D.C., 2018. Second Harmonic Generation Signals
858 in Rabbit Sclera As a Tool for Evaluation of Therapeutic Tissue Cross-linking (TXL) for Myopia. *J Vis
859 Exp*, 56385.10.3791/56385

860

Supplementary Materials

1. Composition of the films: screening phase

In the screening phase, two different types of hyaluronic acid were considered (300 vs 1000 kDa), as well as two PVAs, characterized by a similar MW, but with a different hydrolysis degree (87% vs 98%), that confers peculiar properties to this polymer. As plasticizer, PEG 400 and glycerin were tested. At first, films flexibility and films texture/handling were evaluated. The evaluation was carried out through simple visual inspection and manipulation, to figure out if the film was easily handled and, at the same time, if it had adequate flexibility to be applied to ocular tissues (too rigid materials can cause mechanical damage).

The film compositions evaluated in the screening phase are summarized in Table S1.

Briefly, films made by PVA only (both 87 and 98) were very stiff. The addition of HA (50:50 weight ratio) increased their flexibility, regardless of the MW of the hyaluronan used (300 vs 1000 kDa). HA with a MW of 1000 kDa was selected for further studies, due to the better texture of the film and the higher performance reported in the literature for ocular surface hydration and lubrication, as a result of an effective maintenance of secreted mucin of the ocular surface [1, 2]. To further increase film flexibility, glycerin and PEG 400, both plasticizers approved for ocular application [3], were tested. The best result in terms of flexibility was obtained with 10% glycerin. Finally, to improve the film texture and handling, the HA:PVA ratio was brought to 40:60.

After the screening phase, two different films were selected for further experiments (#12 and #13, Table S1): they both contained a HA:PVA:glycerin in ratio 36:54:10 and differed for PVA grade (98 vs 87).

Table S1. Composition of the blank films prepared with their codification and main features.

#	Components			Weight ratio HA/PVA/PLAST	Flexibility	Texture/ handling		CODE (further used in the paper)
	HA ^a	PVA ^b	Plast ^c					
1	-	87	-	-	-	++++		
2	-	98	-	-	-	++++		
3	300	87	-	50/50	+	++		
4	300	98	-	50/50	+	++		
5	1000	87	-	50/50	+	++		
6	1000	98	-	50/50	+	++		
7	1000	87	Glycerin	47.5/47.5/5	++	++		
8	1000	98	Glycerin	47.5/47.5/5	++	++		
9	1000	87	Glycerin	45/45/10	+++	++		
10	1000	98	Glycerin	45/45/10	+++	++		
11	1000	98	PEG 400	45/45/10	+/-	++		
12	1000	87	Glycerin	36/54/10	+++	+++	<i>Selected formula</i>	87
13	1000	98	Glycerin	36/54/10	+++	+++	<i>Selected formula</i>	98

^a polymer MW

^b % of hydrolysis

^c plasticizer

2. Hyaluronic Acid quantification

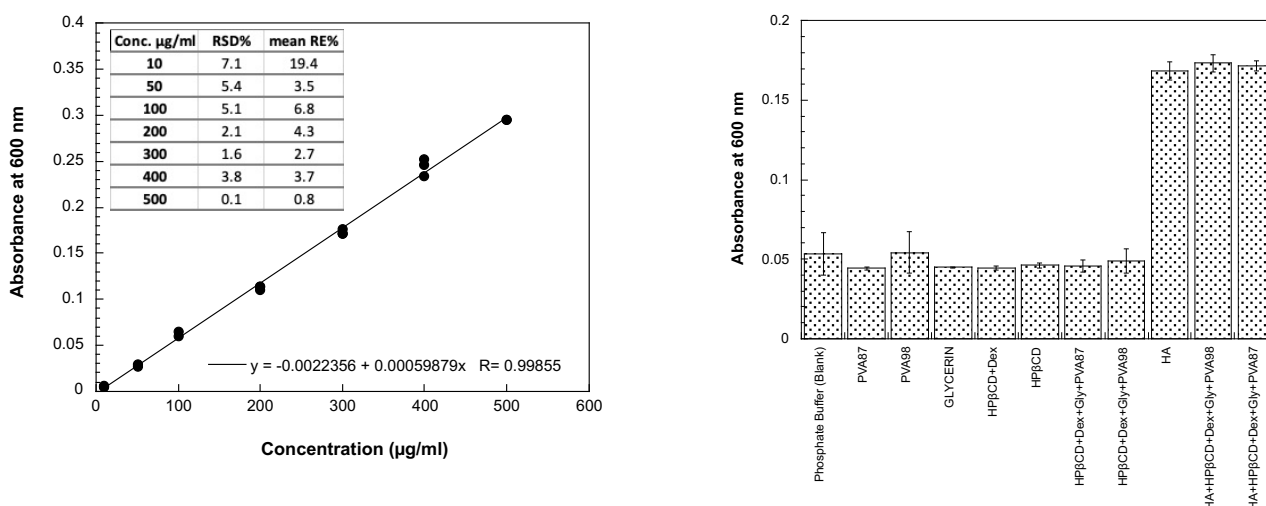
The method was adapted from a previous work [4]. Briefly, CTAB reagent (1.25 g) was dissolved in 50 ml of 2% (w/v) NaOH solution. A solution of HA at concentration of 1 mg/ml was prepared in 0.1 M phosphate buffer pH 7.4 and then diluted to obtain the standard concentrations used for the preparation of the calibration curve (see Figure S2).

100 µl of HA standard solution were introduced in a 96-well plate and incubated for 15 minutes at 37°C. Afterwards, 100 µl of CTAB were added and the plate was incubated again for 10 minutes at 37°C. After 20

seconds shaking, absorbance was measured at 600 nm wavelength against blank (0.1 M phosphate buffer pH 7.4) and plotted against HA concentrations for the construction of the calibration curve. Selectivity of the

method was evaluated by preparing solutions containing the different components of the films, alone or combined (Figure S2).

For the quantification of HA in the film, the punched films (0.6 cm² of area) were dissolved in 10 ml of 0.1 M phosphate buffer pH 7.4. Afterwards, 1 ml of solution was withdrawn, centrifuged (12 minutes at 12000 rpm) and/or filtered (0.22 μm) and analyzed with the method described above.



Film	HA % in the film	Calculated %
# 12 beta (PVA87)	~25	50.94±14.05
# 13 beta (PVA 98)	~25	65.19±4.92

Figure S1. Analytical method for hyaluronic acid quantification. Panel A: Calibration curve and related parameters. The concentration range has been selected on the basis of the expected concentrations in a release study. Panel B. Study of the possible interference of the film components on the absorbance of an HA sample (conc about 200 μg/ml). The concentration of the other components has been selected based on HA/component ratio in the film. The method is selective for HA, the presence of PVA, glycerin and cyclodextrins do not interfere with the analysis. Panel C. Quantification of HA in the film using the previously validated method. The film (0.6 cm²) was dissolved in 10 ml of phosphate buffer (PB). The result suggests that, after drying, an interaction between HA and the other components takes place, preventing the use of this method for quantification of HA release from the film.

3. Drug retention inside the cornea

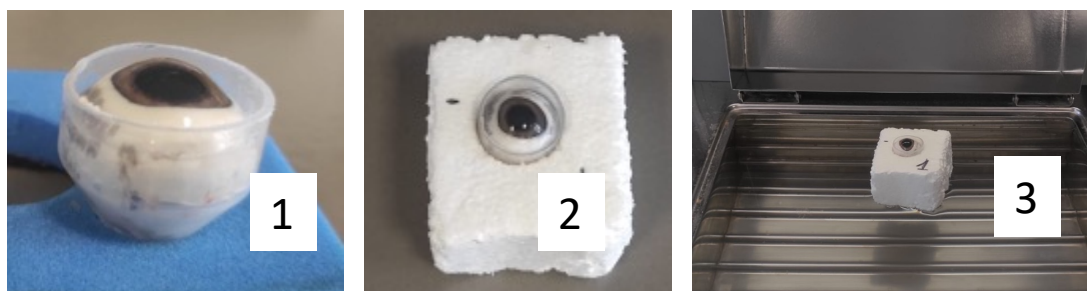


Figure S2. Set-up for the corneal retention experiment using intact eye bulbs. 1) Conical plastic falcons were cut at the bottom and filled with 1 ml of saline solution. The eye bulb was inserted in the falcon with the cornea facing up 2) The

falcon was placed into a floating polystyrene support. 3) Then, the film was applied and the system was inserted inside a bath at 37°C for 4 h, covered with a lid to keep a relative high RH% on eye surface.

Table S2. Comparison between DEX corneal accumulation starting from different films. The table reports the *p* values obtained (*t*-test) from the comparison of the values reported in Table 3 of the main text.

	87_βDL	98_βDL	98_βD	87_βD	87_ββD
87_βDL		0.8098	0.5313	0.2294	0.1241
98_βDL	0.8098		0.2242	0.1109	0.0422
98_βD	0.5313	0.2242		0.0096	0.0053
87_βD	0.2294	0.1109	0.0096		0.1087
87_ββD	0.1241	0.0422	0.0053	0.1087	

4. Two-photon microscopy spectra

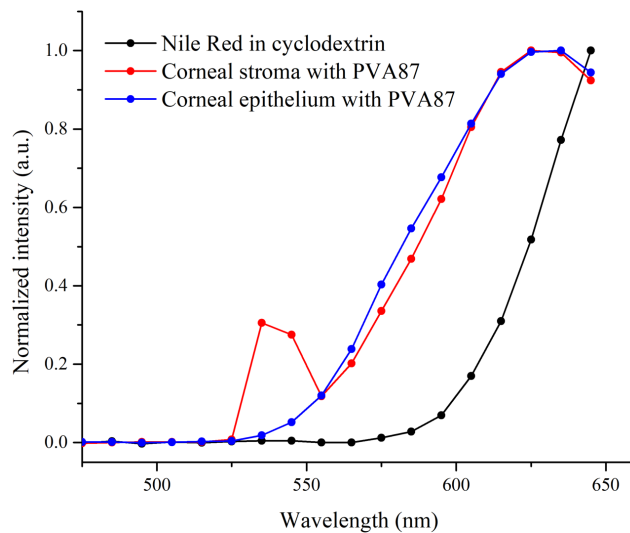


Figure S3. Emission spectra recorded in tissue samples and in solution. Spectra were collected exciting the sample at 1080 nm, in order to minimize the tissue autofluorescence and maximize at the same time the NR signal. Spectra collected with the multiphoton microscope are limited to 650 nm, since higher wavelengths fall out of the detectable range of the instrument.

5. References

- [1] T. Kojima *et al.*, "The Effects of High Molecular Weight Hyaluronic Acid Eye Drop Application in Environmental Dry Eye Stress Model Mice," (in eng), *International journal of molecular sciences*, vol. 21, no. 10, p. 3516, 2020, doi: 10.3390/ijms21103516.
- [2] R. Beck, O. Stachs, A. Koschmieder, W. G. K. Mueller-Lierheim, S. Peschel, and G. B. van Setten, "Hyaluronic Acid as an Alternative to Autologous Human Serum Eye Drops: Initial Clinical Results with High-Molecular-Weight Hyaluronic Acid Eye Drops," *Case Reports in Ophthalmology*, vol. 10, no. 2, pp. 244-255, 2019, doi: 10.1159/000501712.
- [3] "US Food and Drug Administration, Database of Inactive Ingredients."

- [4] N. Oueslati *et al.*, "CTAB turbidimetric method for assaying hyaluronic acid in complex environments and under cross-linked form," *Carbohydrate Polymers*, vol. 112, pp. 102-108, 2014/11/04/ 2014, doi: <https://doi.org/10.1016/j.carbpol.2014.05.039>.